Annals of Anatomy 240 (2022) 151881

Contents lists available at ScienceDirect

Annals of Anatomy

journal homepage: www.elsevier.com/locate/aanat

Research article

Can domestication shape Canidae brain morphology? The accessory olfactory bulb of the red fox as a case in point

Irene Ortiz-Leal [1], Mateo V. Torres [1], Paula R. Villamayor, Luis Eusebio Fidalgo, Ana López-Beceiro, Pablo Sanchez-Quinteiro *

Department of Anatomy, Animal Production and Clinical Veterinary Sciences, Faculty of Veterinary, University of Santiago de Compostela, Lugo, Spain

ARTICLE INFO

Article history:
Received 22 August 2021
Received in revised form 2 December 2021
Accepted 3 December 2021
Available online 9 December 2021

Keywords:
Vomeronasal system
Accessory olfactory bulb
Fox
Canidae
Immunohistochemistry
Lectins
UEA
G proteins

ABSTRACT

Background: The accessory olfactory bulb (AOB) is the first integrative center of the vomeronasal system (VNS), and the general macroscopic, microscopic, and neurochemical organizational patterns of the AOB differ fundamentally among species. Therefore, the low degree of differentiation observed for the dog AOB is surprising. As the artificial selection pressure exerted on domestic dogs has been suggested to play a key role in the involution of the dog VNS, a wild canid, such as the fox, represents a useful model for studying the hypothetical effects of domestication on the AOB morphology.

Methods: A comprehensive histological, lectin-histochemical, and immunohistochemical study of the fox AOB was performed. Anti-Gαo and anti-Gαi2 antibodies were particularly useful, as they label the transduction cascade of the vomeronasal receptor types 1 (V1R) and 2 (V2R), respectively. Other employed antibodies included those against proteins such as microtubule-associated protein 2 (MAP-2), tubulin, glial fibrillary acidic protein, growth-associated protein 43 (GAP-43), olfactory marker protein (OMP), calbindin, and calretinin.

Results: The cytoarchitecture of the fox AOB showed a clear lamination, with neatly differentiated layers; a highly developed glomerular layer, rich in periglomerular cells; and large inner cell and granular layers. The immunolabeling of Gαi2, OMP, and GAP-43 delineated the outer layers, whereas Gαo and MAP-2 immunolabeling defined the inner layers. MAP-2 characterized the somas of AOB principal cells and their dendritic trees. Anti-calbindin and anti-calretinin antibodies discriminated neural subpopulations in both the mitral-plexiform layer and the granular cell layer, and the lectin *Ulex europeus* agglutinin I (UEA-I) showed selectivity for the AOB and the vomeronasal nerves.

Conclusion: The fox AOB presents unique characteristics and a higher degree of morphological development compared with the dog AOB. The comparatively complex neural basis for semiochemical information processing in the fox compared with that observed in dogs suggests loss of AOB anatomical complexity during the evolutionary history of dogs and opens a new avenue of research for studying the effects of domestication on brain structures.

1. Introduction

Animals have acquired complex chemical communication systems through evolution, enabling them to interact with the external environment, recognize a large variety of chemical cues and translate these cues into sensory information (Wyatt, 2003). Olfaction involves two primary systems: the main olfactory system (MOS) and the less studied accessory olfactory system, also known as the vomeronasal system (VNS) (Jezierski et al., 2016; McLean et al., 2021). The VNS is essential for animal well-being, providing fundamental information used in predator detection (Papes et al., 2010), maternal recognition (Del Cerro, 1998) and non-conscious sexual and social behaviors (Clancy et al., 1984; Martínez-Ricós et al., 2008; Pardo-Bellver et al., 2017; Pallé et al., 2020). The VNS is comprised of the vomeronasal organ (VNO), a tubular sensory structure; the accessory olfactory bulb (AOB), the first integration system of the VNS pathway; and the vomeronasal amygdala (Holy, 2018). Vomeronasal nerves connect the VNO with the AOB, providing functionality

* Correspondence to: Department of Anatomy, Animal Production and Clinical Veterinary Sciences, Faculty of Veterinary, University of Santiago de Compostela, Av Carballo Calero s/n, 27002 Lugo, Spain.
E-mail address: pablo.sanchez@usc.es (P. Sanchez-Quinteiro).
[1] I.O.L. and M.V.T. are joint first authors.

https://doi.org/10.1016/j.aanat.2021.151881
0940-9602/

(Salazar and Sánchez-Quinteiro, 2009). In contrast with the conscious response generated in the MOS, the VNS is only connected to limbic system centers and specific regions of the hypothalamus and it is not known to be associated with any higher cognitive structures of the brain (Halpern, 1987; Gutiérrez-Castellanos et al., 2014). Therefore, the VNS is not thought to result in the conscious perception of the detected chemical molecules.

Despite the anatomical proximity between these two olfactory systems, these systems have historically been viewed as independent, with large morphofunctional differences, suggesting independent evolutionary pathways (Wysocki, 1979; Halpern and Martínez-Marcos, 2003; Barrios et al., 2014). Differences can be observed across physiological, behavioral, and morphofunctional aspects between these two systems, especially the morphofunctional diversity observed for the VNS among mammal families (Meisami and Bhatnagar, 1998; Salazar et al., 2007; Torres et al., 2020). Therefore, the interspecies extrapolation of anatomical and histological information for the VNS can be difficult and result in imprecise information (Salazar and Sánchez-Quinteiro, 2009).

Despite the large degree of diversity found in the VNS, the VNO presents a common, general morphological pattern across species within Mammalia. In the AOB, however, fundamental differences in the general macroscopic, microscopic, and neurochemical organizational patterns have been reported between species (Frahm and Bhatnagar, 1980; Switzer et al., 1980; Meisami and Bhatnagar, 1998). For example, the degree of differentiation in the AOB differs widely within the Carnivora order, even when comparing families that are closely related. The cat (*Felis silvestris catus*) and the dog *(Canis lupus familiaris)* present two very different degrees of differentiation. The cat AOB is well developed and presents clearly defined layers within the AOB (Salazar and Sánchez-Quinteiro, 2011). However, the dog presents a surprisingly low degree of differentiation (Salazar et al., 1994 and 2013; Nakajima et al., 1998), which has long been a point of open discussion, given the well-known roles played by pheromonal chemosensory and the highly social behaviors observed in this species (Pageat and Gaultier, 2003; Kaminski and Marshall-Pescini, 2014). Ramón y Cajal (1902) concluded that dogs did not present a structure that could be defined as the AOB. Several decades later, Jawlowski (1956) and Miodonski (1968) identified a presumptive AOB in canids through the examination of histological sections. Although these studies were not conclusive, and only included drawings, and not pictures, their descriptions correspond with the description given by Salazar et al. (1992), who characterized the dog AOB using lectin-histochemical studies and verified the direct connection between the AOB and the vomeronasal nerves and VNO, demonstrating its unequivocal presence for the first time. The existence of the AOB in dogs was later confirmed by Nakajima et al. in 1998.

The artificial selection pressure exerted on domestic dogs has been suggested to play a key role in the involution of its olfactory and vomeronasal systems. However, whether this involution is due to domestication or whether a poorly developed VNS occurs independently of domestication remains unclear. The examination of phylogenetic ancestors of the dog, such as the wolf, or the study of other wild canids, such as the fox, is necessary to determine whether poor differentiation is specific to dogs. Although the wolf would be the ideal comparative model for studying the effects of domestication on the VNS in the dog, given their phylogenetic proximity (Skoglund et al., 2015), no studies have been reported examining the VNS in the wolf, and the availability of wolf samples in good condition for these studies is very low. The fox is a convenient and useful model for the morphofunctional study of the AOB of wild canids, given the phylogenetic proximity between the fox (*Vulpes vulpes*) and the dog (*Canis familiaris*), which diverged only 10 million years ago from a common ancestor (Graphodatsky et al., 2008), making these species good candidates for the study of domestication. The studies reported by Kukekova et al. (2014); Wang et al. (2018) in foxes selected for tame behavior have led to the hypothesis that the domesticated behaviors observed in dogs and foxes may have similar genetic bases, making the fox an excellent model for studying the genetics of domestication in canids.

For this reason, we have approached this issue by examining a wild canid, the red fox (*Vulpes vulpes*), for which only the VNO component of the primary vomeronasal system has been characterized (Ortiz-Leal et al., 2020), identifying in this study specific and noticeable differences in the VNS of the fox compared with that of the dog. Specifically, both anti-Gαo and anti-Gαi2 subunits were positively immunolabeled in the VNO epithelium of the fox. In most Rodentia family species, which have historically been used as a reference for VNO studies in mammals (Salazar et al., 2013), the neuroepithelium of the VNO expresses two distinct G proteins: Gαi2, found in the apical neurosensorial layer, associated with the expression of type 1 vomeronasal receptor families (V1R), and in neurons that project to the anterior region of the AOB (Berghard and Buck, 1996); and Gαo protein, complementarily expressed in the basal portion of the neurosensorial neuroepithelium, associated to the expression of type 2 vomeronasal receptor families (V2R), and in neurons that project to the posterior region of the AOB (Herrada and Dulac, 1997; Matsunami and Buck, 1997; Ryba and Tirindelli, 1997). The immunopositive characterization of both Gαi2 and Gαo have been considered excellent phenotypic indicators of V1R and V2R expression in the VNO. However, in other mammals, such as goat (Takigami et al., 2000), sheep (Salazar et al., 2007), dogs (Salazar et al., 2013), and cats (Salazar and Sánchez-Quinteiro, 2011), this differential expression of G proteins has not been observed in either the VNO or the AOB, with the exception of the fox, in which the expression of both Gαi2 and Gαo subunits in the neurosensory epithelium of the VNO was recently identified by our group (Ortiz-Leal et al., 2020). The extended study of Gαi2 and Gαo subunit expression in the fox AOB is, therefore, of great interest.

The aim of the present study was to describe the general features of the fox AOB at both macroscopic and microscopic levels and widen the morphofunctional understanding of the fox AOB, with a focus on positive immunolabeling for anti-Gαo found in the VNO by Ortiz-Leal et al. (2020). A variety of tissue dissection and microdissection techniques, general and specific histological stainings, lectin-histochemical and immunohistochemical labeling techniques were employed.

2. Methods

2.1. Samples

5 foxes were used for this study, supplied from hunting activities organized by the Galician Hunting Federation, with the necessary permissions by the Galician Environment, Territory and Tenement Council. The animals were obtained in the field, the same day of their shot, with a maximum of two hours delay, and immediately transported to the premises of the Veterinary Faculty of Lugo, where the whole olfactory bulbs of all foxes were extracted with the help of an electric plaster cutter and a gouge clamp and conserved in either 10% formalin or Bouin´s fixative (Bf). Details of the foxes processed, and fixatives used are included in Table 1.

Afterwards, the olfactory bulbs were embedded in paraffin wax and serially cut by a microtome either horizontally or in a sagittal plane along its entire length with a thickness of 6–7 µm. Sample sections were stained using haematoxylin-eosin, Nissl, Tolivia and Bielschowsky stains, and lectin histochemical and immunohistochemical techniques.

In one of the individuals, a topographic histological study was conducted on the olfactory bulbs and the olfactory and vomeronasal nerves located in the ethmoidal fossa. After removing the skin,

Table 1
Summary of the foxes, description and fixative used.

Fox	Description	Fixative
Z1	♀ Adult	Bouin's
Z2	♂ Elderly	Bouin's
Z3	♂ Adult	Bouin's
Z5	♂ Young	Formalin
Z7	♀ Young	Bouin's

superficial muscles, mandible, and eyeballs, two transverse cuts were made using a rotary saw to completely delimit the orbital region. The obtained sample was decalcified by immersion in a decalcifying solution (Shandon TBD-1 Decalcifier, ThermoFisher, Pittsburgh, PA) for 8 days at room temperature with continuous stirring. Transverse sections were performed with a microtome blade to obtain 1-cm-thick sections that included the medial surface of the olfactory bulbs and the surrounding ethmoidal turbinates. These samples were washed in running water for 2 h, paraffin embedded, and serially cut into 6-µm-thick sections, which were collected on large microscope slides (76 × 52 mm). Immunohistochemical procedures, including anti-Gαi2, anti-Gαo, and LEA lectin histochemical labeling, were performed the following day on three consecutive sections.

Additionally, for the purposes of performing a comparative assessment of the structural differences between the accessory olfactory bulbs in the dog and fox, we processed olfactory bulb samples from two dog brains obtained from the brain collection of the Unit of Anatomy of the Faculty of Veterinary Sciences of Lugo. Both samples were obtained from adult individuals with no evidence of neurological symptoms or lesions. The samples were fixed and processed in an identical manner as the fox samples and were stained with Nissl and Tolivia stains and immunohistochemically labeled with anti-Gαo antibody.

2.2. Tolivia protocol

Sections were deparaffinized and hydrated. Then, sections were mordanted for 1 h in 2.5% $(SO_4)_2FeNH_4$, then washed for 1 min in distilled water. Myelin staining was achieved after 2.5 h immersion in a freshly made solution: 50 ml of 50% ethanol to which 5 ml of 20% hematoxylin and 10 ml of 1% Li_2CO_3 was added. Sections were then washed for 3 × 5 min prior to staining for 5 min in the following solution: 0.2% pyronine and 20% formaldehyde. The slides were finally dehydrated, cleared and mounted (Tolivia et al., 1988).

2.3. Bielschowsky's silver stain protocol

Slides were deparaffinized and hydrated, then stained in 20% silver nitrate ($AgNO_3$) in the dark at 37 °C for 30 min and washed in distilled water for 2 × 5 min. Concentrated ammonia was slowly added to the $AgNO_3$ solution to dissolve the precipitate formed. Then, slides were introduced in this solution for 15 min at 37 °C in the dark, and posteriorly washed in 2 × 10 min 0.1% ammonia washes. A developer solution (20 ml 10% formaldehyde, 0.5 g citric acid and 2 drops of nitric acid in 100 ml distilled water) was added to the silver solution. Slides where then washed in the solution for 10 min, washed again in ammonia and submerged in 5% sodium thiosulfate ($Na_2S_2O_3$) for 1 min. Finally, samples were washed in distilled water, dehydrated, cleared and mounted.

2.4. Lectin histochemistry staining

Three different lectins were used: *Ulex europaeus* agglutinin I UEA-I, which specifically labels the VNS pathway in several species, including the dog (Salazar et al., 1992); *Lycopersicon esculentum* agglutinin (LEA), which labels both the main and accessory olfactory systems (Salazar et al., 2019); and *Bandeiraea simplicifolia* isolectin B_4 ($BSI-B_4$), which specifically labels the VNS pathway in rats (Ichikawa et al., 1992; Salazar and Sánchez Quinteiro, 1998) and opossums (Shapiro et al., 1995).

2.4.1. LEA and BSI-B_4 protocol

Before proceeding with the lectin histochemistry protocol, all sample slides were deparaffinized and rehydrated. Biotinylated conjugates of LEA and $BSI-B_4$ were used for this study (see details in Table 2). Firstly, 3% hydrogen peroxide (H_2O_2) solution was used to inactivate endogenous peroxidase activity. Then sections were incubated in a 2% bovine serum albumin (BSA) in 0.1 M phosphate-buffered (pH 7.2) solution (PB). Slides were then incubated overnight with LEA and $BSI-B_4$ lectins, independently, in a 0.5% BSA solution. After the incubation, the samples were washed 2 × 2 min in PB, and afterwards incubated during 1.5 h at room temperature with avidin-biotin-peroxidase complex (ABC) reagent (Vectastain; Vector Laboratories, Burlingame, CA, USA). To visualize the reaction, a 0.05% 3,3'-diaminobenzidine (DAB) chromogen solution and a 0.003% H_2O_2 solution, in 0.2 M Tris-HCl buffer solution were used. The DAB reagent develops into a brown precipitate in the presence of the hydrogen peroxide solution, which enables the visualization of the reaction.

2.4.2. UEA-I protocol

As with the LEA and $BSI-B_4$ lectins, before the lectin histochemistry protocol, it is necessary to deparaffinize, rehydrate the slides and incubate the samples with 3% H_2O_2 solution to inactivate endogenous peroxidase activity. The samples were then incubated for 1 h at room temperature in a 0.5% BSA/UEA-I solution and then washed for 3 × 5 min in a PB solution. The slides where then incubated overnight with an anti-UEA-I peroxidase-conjugated antibody. The next day, the samples were washed with a PB solution. A DAB solution was added to visualize the reaction.

Controls were performed for both protocols, both without the addition of lectins and with the preabsorption of lectins, by using an excess amount of the corresponding sugar.

2.5. Immunohistochemical staining

A thorough immunohistochemical study was performed to study the fox olfactory bulb. Among the antibodies used (Table 2), the anti-Gαo and anti-Gαi2 antibodies are particularly useful because they label the transduction cascade for V2R and V1R vomeronasal receptors, respectively. Neuronal dendritic formation in the bulb was characterized employing microtubule-associated protein 2 (MAP-2) and α-tubulin antibodies. Astrocytes and ensheathing cells were identified using antibodies against glial fibrillary acidic protein (GFAP). Neuronal axonal growth and synaptogenesis were characterized by using an anti-growth-associated protein 43 (GAP43) antibody. Antibodies were also used to detect olfactory marker protein (OMP), which is expressed in mature neurons in both olfactory subsystems. The immunohistochemical study was conducted by examining the expression patterns of the calcium-binding proteins calbindin (CB) and calretinin (CR), which participate in the regulation of cytosolic free calcium ion concentrations in neurons. The distribution of calcium-binding proteins has previously been recognized as a useful neuronal marker for identifying specific brain regions and discrete neuronal subpopulations (Coppola and Disney, 2018; De Góis Morais et al., 2021).

2.5.1. Antibody characterization and specificity

Information for all antibodies, including sources, dilutions used, target immunogens, and Research Resource Identifiers (RRID), are presented in Table 2. In all cases, the immunostaining patterns

Table 2
Detailed information on the antibodies and lectins used in this study.

Antibody	1st Ab species / dilution	1st Ab catalog number	Immunogen	Reference	RRID	2nd Ab species/dilution, catalog number
Anti-Gαo	Rabbit 1:200	Santa Cruz Biotechnology sc-387	Peptide mapping within a highly divergent domain of Gαo of rat origin	Torres et al. (2021)	AB_2111641	ImmPRESS VR HRP Anti-rabbit IgG Reagent MP-6401–15
Anti-Gαo	Rabbit 1:200	MBL-551	Bovine GTP Binding Protein Gαo subunit	Prince et al. (2009)	AB_591430	ImmPRESS VR HRP Anti-rabbit IgG Reagent MP-6401–15
Anti-Gαi2	Rabbit 1:200	Santa Cruz Biotechnology sc-7276	Peptide mapping within a highly divergent domain of Gαi2 of rat origin	De la Rosa-Prieto et al. (2010)	AB_2111472	ImmPRESS VR HRP Anti-rabbit IgG Reagent MP-6401–15
Anti-OMP	Goat 1:400	Wako 544–10001	Rodent olfactory marker protein	Koo et al. (2005)	AB_2315007	Horse anti-goat IgG 1:250 Vector BA-9500
Anti-GAP-43	Mouse 1:4000	Sigma G9264	Mouse clone GAP-7B10	Gonzalez-Lozano et al. (2016)	AB_477034	ImmPRESS VR HRP Anti-mouse IgG Reagent MP-6402–15
Anti - CB	Rabbit 1:6000	Swant CB38	Rat recombinant calbindin D-28k	Hermanowicz-Sobieraj et al. (2018)	AB_10000340	ImmPRESS VR HRP Anti-rabbit IgG Reagent MP-6401–15
Anti-CR	Rabbit 1:6000	Swant 7697	Recombinant human calretinin containing a 6-his tag at the N-terminus	Adrio et al. (2011)	AB_2619710	ImmPRESS VR HRP Anti-rabbit IgG Reagent MP-6401–15
Anti–MAP-2	Mouse 1:400	Sigma M4403	Rat brain microtubule-associated proteins	Kotani et al. (2010)	AB_477193	ImmPRESS VR HRP Anti-mouse IgG Reagent MP-6402–15
Anti-GFAP	Rabbit 1:400	Dako Z0334	GFAP from bovine spinal cord	Shibata et al. (2013)	AB_10013382	ImmPRESS VR HRP Anti-rabbit IgG Reagent MP-6401–15
Anti-α-tubulin	Rabbit 1:500	Abcam 7291	Full length native protein (purified) corresponding to chicken α-tubulin	Nawaz et al. (2020)	AB_2241126	ImmPRESS VR HRP Anti-mouse IgG Reagent MP-6402–15
UEA	1:60	Vector L-1060				Rabbit 1:50 DAKO P289
LEA	20 µm/ml	Vector B-1175				Vectastain ABC reagent PK-4000
BSI-B_4	100 µm/ml	Sigma L-2140				Vectastain ABC reagent PK-4000

Abbreviations: ABC, avidin-biotin complex; BSI-B_4, *Bandeiraea simplicifolia* isolectin B_4; CB, calbindin; CR, calretinin; GAP-43, growth-associated protein 43; GFAP, glial fibrillary acidic protein; HRP, horseradish peroxidase; LEA, *Lycopersicon esculentum* lectin; MAP-2, microtubule-associated protein 2; OMP, olfactory marker protein; UEA, *Ulex europaeus* agglutinin.

obtained using these antibodies in the red fox were consistent with prior immunostaining patterns obtained in a variety of mammalian species. Relevant references for each antibody are indicated in Table 2.

2.5.2. Immunohistochemical protocol

Before the immunohistochemical reaction, deparaffinized and rehydrated samples were incubated for 15 min in a 3% H_2O_2 solution to inactivate endogenous peroxidase activity. Either 2.5% horse normal serum of the ImmPRESS reagent kit Anti-mouse IgG/Anti-rabbit IgG (Vector Laboratories, Burlingame, CA, USA) or 2% BSA was used for 30 min to block non-specific binding sites (Table 2). The samples were then incubated with the primary antibody at 4 °C overnight and under humid conditions. Samples previously blocked with the ImmPRESS kit were incubated for 20 min with either the ImmPRESS VR Polymer HRP Anti-Rabbit IgG or the Anti-mouse IgG reagent (Table 2), except for the slides incubated with the anti-OMP antibody (raised in goat), which were incubated with a biotinylated anti-goat IgG for 1.5 h, and then incubated in ABC reagent. In all cases, successive 3 × 3 min PB washes were performed in between steps. Finally, slides were rinsed in 0.2 M Tris-HCl, pH 7.61 for 10 min before developing with a DAB chromogen (same protocol as for the lectin histochemical labeling), and then dehydrated and mounted.

For all immunohistochemical procedures, the omission of the primary antibody was used as a negative control, and no labeling or non-specific background staining was observed for any negative control samples. As positive controls, we replicated the immunohistochemical procedure in previously unstained mouse or rabbit tissue obtained during previous experiments. These samples were known to express the proteins of interest, and the expected positive results were obtained in all cases.

2.6. Image acquisition and digital processing

Images were captured with a Karl Zeiss Axiocam MRc5 digital camara coupled to a Zeiss Axiophot microscope. Brightness, contrast and balance levels were adjusted using Adobe Photoshop CS4 (Adobe Systems, San Jose, CA, USA). No specific characteristics within the images were altered, enhanced, moved or introduced.

3. Results

The study of the AOB will be addressed at both the macroscopic and microscopic levels.

3.1. Macroscopic study of the accessory olfactory bulb

The fox MOBs are located inside the ethmoidal fossa and were extracted in conjunction with the brain in our specimens (Fig. 1A and B). Visual inspection revealed well-developed bulbs, similar to those observed in dogs, although the fox olfactory bulbs appear to be more elongated in the dorsoventral axis (Fig. 1C–F). The AOB was not visible at first glance, although following the removal of the rostral-most section of the frontal lobe, we noted a small ovoid protuberance on the posterior third of the medial edge of the MOB, which we presumed to be the location of the AOB (asterisk in Fig. 1D) and was later confirmed by histological serial sectioning of the whole olfactory bulb.

The remaining anatomical structures that constitute the olfactory pathway also presented remarkable development, including the lateral olfactory tract (LOT), olfactory tubercle (OT), and piriform lobe (Pyr) (Fig. 1B).

3.2. Microscopic study of the accessory olfactory bulb

3.2.1. Histological and immunohistochemical features

The microscopic study of the olfactory bulb confirmed the presence of an AOB in the fox, located in a caudoventral position, relative to the MOB (Fig. 2A, and D–F). Hematoxylin and eosin (HE) and Nissl stainings were used to study the texture of the AOB, through which the AOB layering could easily be identified (Fig. 2B and C). From the superficial to deep planes, the following layers were discernible: vomeronasal nerve (Vn), glomerular (Glm), mitral-plexiform (M-P), and granular (Gr) layers (Fig. 2B). The nervous and glomerular layers appear particularly well-developed in this species. The periglomerular cells formed many irregular, tortuous strands (Fig. 3A); therefore, the glomeruli did not present with well-defined margins. Occasionally, larger neurons with rounded nuclei, presumably interneurons, could be located in the innermost part of the glomerular layer.

Instead of the monolayer of mitral cells typically observed in the MOB, the principal cells of the AOB are scattered along a patch of neuropil, which extends from the glomerular (Glm) to the granular layers of the AOB (Figs. 2B and 3D), referred to as the mitral-plexiform layer (M-P) layer. This layer is well-defined, and its central part deepens into approximately the middle portion of the Glm. The arrangement of the principal cells can be clearly observed by immunohistochemical and histochemical labeling (Figs. 4–6). The number of principal cells is abundant, and they are arranged in parallel along the anteroposterior axis of the AOB.

These principal cells display either miter or ellipsoid shapes and have large soma containing large, rounded nuclei and patent nucleoli (Fig. 3B and F). Between the principal cells, numerous smaller cells can be observed, containing round nuclei and cytoplasm, featuring barely noticeable prolongations. These cells presented with differing neurochemical patterns compared with the principal cells (Fig. 3H–M). The granular layer (Fig. 2B) was comprised of typical clusters of small, rounded granule cells, surrounded by larger isolated multipolar neurons (Fig. 3C).

Both Bielschowsky (Fig. 2D and G) and Tolivia (Fig. 2F, H, and I) stains enabled the identification of both the main cell types and myelinated nerve fibers contained in the fox AOB. The presence of a wide tract of myelinated fibers along the anteroposterior axis of the AOB and delimiting the mitral-plexiform and granular layers is noteworthy and represents the contribution of the AOB to the LOT (Fig. 2D, F, and I). These fibers extend horizontally and perpendicularly toward the granular layer (Fig. 3D and E), with reducing density toward the mitral cell band (Fig. 3E and F), occupying the spaces left free by the principal and granular cells of both layers. Additionally, these stains showed an atypical glomerular formation, consisting of an isolated glomerulus located in the caudal portion of the AOB, surrounded by myelinated fibers and differentially stained (Fig. 2G and H).

Several antibodies against different proteins were used to study the fox AOB. Anti-Gαi2 specifically labels the i2 family of the G-protein α subunit, which is present in the transduction cascade of the V1R vomeronasal receptor, revealed positive labeling concentrated in the vomeronasal nerve (Vn) and glomerular (Glm) layers (Fig. 4A). By contrast, the mitral-plexiform layer (M-P) did not show immunopositive labeling for anti Gαi2. Anti-Gαo labels a component found in the transduction cascade of the V2R vomeronasal receptor and displayed a complementary pattern, illustrating how the M-P layer deepens into the Glm layer (Fig. 4B). According to our observations in an older fox specimen, this pattern could vary, as shown in Fig. 4D, between older and younger specimens: the arborization pattern observed in the younger specimen was thicker and broader. We did not identify anti-Gαo immunolabeling in the superficial layers of the AOB; therefore, the typical anteroposterior

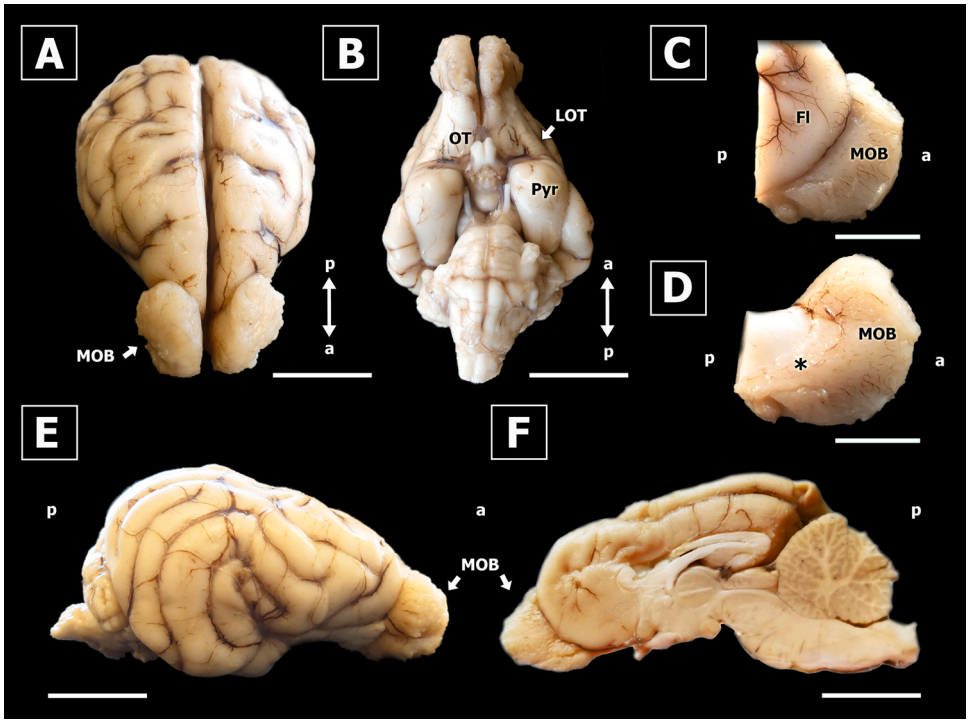

Fig. 1. The brain and main and accessory olfactory bulbs of the fox. A. Rostrodorsal view of the brain. B. Ventral view of the brain, with the main structures of the olfactory pathway indicated: piriform lobe (Pyr), olfactory tubercle (OT), and lateral olfactory tract (LOT). C. Medial view of the left olfactory bulb, covered by the frontal lobe of the telencephalon (Fl). D. Medial view of the left olfactory bulb, after the removal of the rostral portion of the telencephalon. Both the caudomedial surface of the main olfactory bulb (MOB) and the rostral portion of the olfactory peduncle are now visible. The presumptive area of localization for the accessory olfactory bulb is indicated (asterisk). E. Lateral view of the brain. F. Medial view of the right hemiencephalon. a: anterior, p: posterior. Scale bar: A, B, E, F: 2 cm. C, D: 0.5 cm.

zonation found in the species expressing the two families of vomeronasal receptors, V1R and V2R, was also not observed.

The anti-MAP2 antibody, which is a consistent marker for the dendritic branching of mitral cells in all species, shows a similar outcome as observed using the anti-Gαo antibody, with no reactivity in the vomeronasal nerve (Vn) and glomerular (Glm) layers and strong immunopositive labeling in the mitral-plexiform (M-P) and granular layers (Fig. 4C). Higher magnification images of the anti-MAP2 immunostaining (Fig. 3M) confirmed that the labeling was concentrated in the mitral cell somas and their dendritic projections to the Glm layer.

The use of anti-OMP antibody enables the specific labeling of OMP protein, which is associated with mature neurons in both the MOS and VNS. The anti-OMP immunopositive labeling of the fox AOB showed a similar pattern as was observed using the anti-Gαi2 antibody, labeling both the vomeronasal nerve and glomerular layers. MOB glomeruli are more intensely labeled with anti-OMP than those of the AOB (Fig. 5A).

The anti-GAP-43 antibody selectively labels the GAP-43 protein, which is typically found in large quantities in axonal growth cones. This antibody showed immunopositive labeling in the vomeronasal nerve, glomerular and granular layers, whereas the mitral-plexiform layer was immunonegative (Fig. 5B).

The anti-GFAP antibody selectively labels the glial-fibrillar protein, which is located along the entire thickness of the AOB (Fig. 5C). The anti-GFAP labeling observed in the superficial layers of the AOB can be attributed to the profuse arborizations of the ensheathing cells that enclose the nervous fibers of the vomeronasal nerve layer. In the deep layers of the AOB, anti-GFAP labeling characterizes branched astrocytes (Fig. 5F).

Antibodies against cytoplasmic calcium-binding superfamily proteins, including CB-D28k and CR (Fig. 5D and E, respectively), showed intense immunopositive labeling, especially the anti-CR antibody. Anti-CR and anti-CB labeling appeared broadly and diffusely throughout the vomeronasal nerve and glomerular layers of the AOB, whereas the labeling was restricted to small subpopulations of neurons in the mitral-plexiform (M-P) and granular layers. Hematoxylin counterstaining showed that both markers stained only a small fraction of both principal and smaller M-P neurons, staining the soma (Fig. 3H and I for CR; Fig. 3K and L for CB) and, in the case of CB, fine processes (Fig. 3L). The immunolabeling pattern we observed using both CB and CR antibodies did not allow us to discriminate the presence of specific neuronal subpopulations for these two proteins.

3.2.2. Lectin-histochemical study of the AOB

A study of the AOB was performed using the lectins UEA-I and LEA. A specific positive labeling pattern was observed using UEA-I, in which the vomeronasal nerve layer showed weaker labeling than the glomerular layer. The AOB glomeruli configuration could be observed with great clarity using lectin-histochemical staining compared with the pattern observed using general histological stains (Fig. 6A). The vomeronasal nerve (NVN) was also easily distinguished due to positive labeling by UEA-I (Fig. 6A). Both the MOB and the frontal lobe of the telencephalon were negative for UEA-I.

A positive labeling pattern for LEA was observed, concentrating on the vomeronasal nerve and glomerular (Glm) layers of the AOB. The mitral-plexiform and granular layers were negative for LEA (Fig. 6B). In contrast with the pattern observed using UEA-I, LEA labeling showed a strong positive pattern in the superficial layers of the MOB (olfactory nerve and Glm layers). Finally, BSI-B_4 staining did not result in any positive labeling in either the fox AOB or MOB.

3.2.3. Immunohistochemical and lectin-histochemical studies of the vomeronasal nerve

The NVNs travel along the medial surface of the MOB before reaching the AOB. To examine these nerves, we examined serial

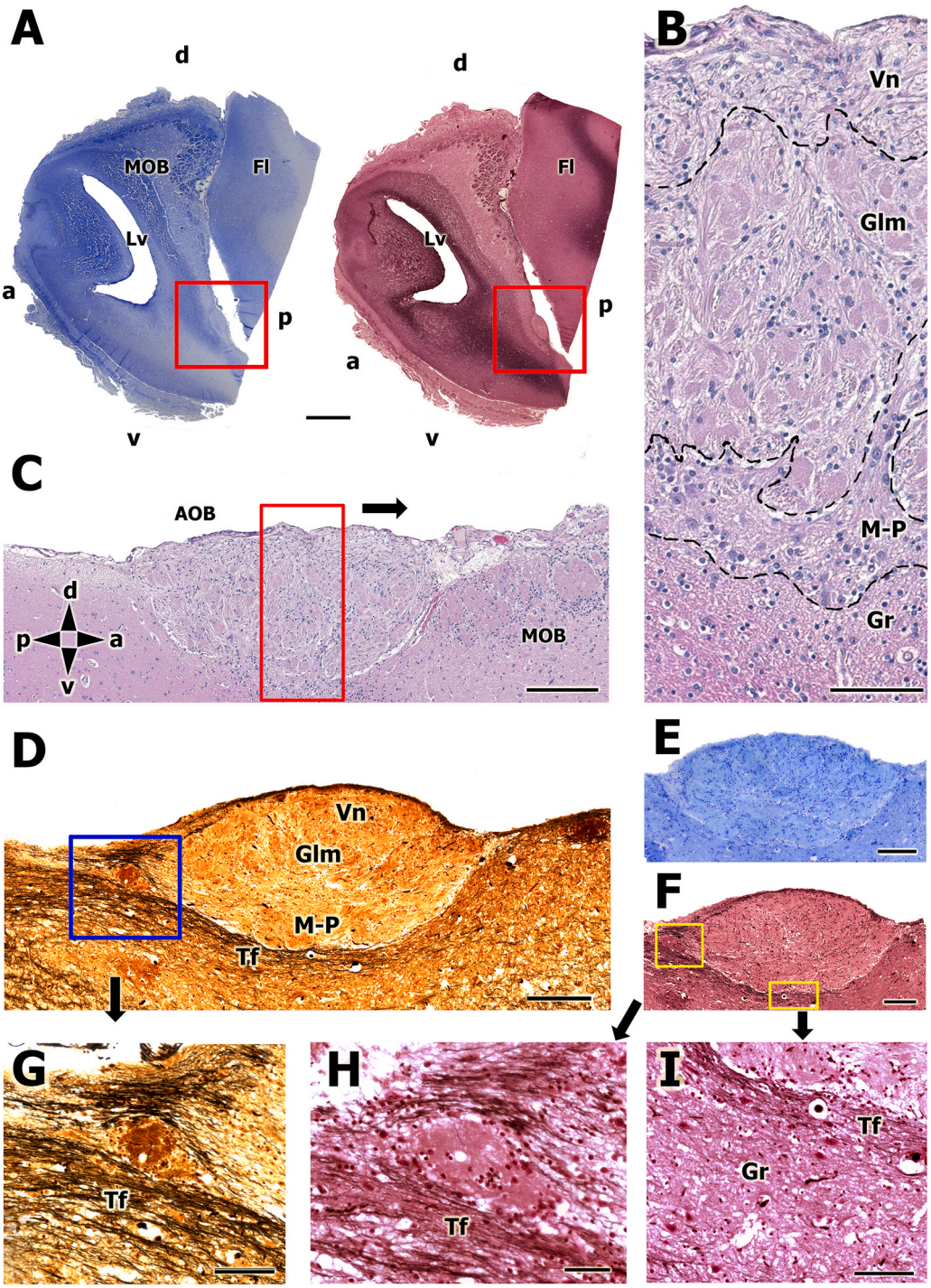

Fig. 2. Histological study of the fox AOB. A. General view of the main olfactory bulb (MOB), cut in the sagittal plane, in which the accessory olfactory bulb (AOB) is framed in red, located in a caudoventral position relative to the MOB. The frontal lobe of the telencephalon (Fl), the MOB, and the lateral ventricle (Lv) can be identified. Nissl and Tolivia stains are shown. B and C. Horizontal sections of the AOB (B corresponds to the red-framed section in C), in which the different layers are identified: nervous layer (Vn), glomerular layer (Glm), mitral-plexiform layer (M-P), and granular layer (Gr). Hematoxylin and eosin stain. D. Sagittal section of the AOB. Bielschowsky stain. The dark brown myelin tract fibers (Tf) are clearly identified. An atypical glomerular formation is framed in blue and shown at higher magnifications in G, surrounded by myelinic fibers. E. Sagittal section of the AOB. Nissl stain. F. Sagittal section of the AOB stained using the Tolivia method, showing another example of an atypical glomerular formation (framed in yellow and shown at higher magnification in H). The tract fibers and the granular layer are also framed in yellow and shown at higher magnification in I. The compass indicates the orientation, as follows: d, dorsal; v, ventral; p, posterior; a, anterior. Scale bars: A: 2 mm. C, D: 250 µm. B, G: 100 µm. E, F: 200 µm. H, I: 50 µm.

decalcified sections of the ethmoidal fossa (Fig. 7A). The olfactory nerves and the superficial layers of the MOB were immunopositive for anti-Gαo; however, this marker did not allow for the identification of the NVN bundle (Fig. 7B). Conversely, anti-Gαi2 staining was only observed in the NVN fascicles in a highly specific manner (Fig. 7C). LEA stained both the olfactory components of the MOB and the NVN (Fig. 7D and G). The presence of small arterioles in a plane deep to the NVN served as a topographic landmark to confirm the anti-Gαo-negative (Fig. 7E) and anti-Gαi2–positive (Fig. 7F) character of the NVN.

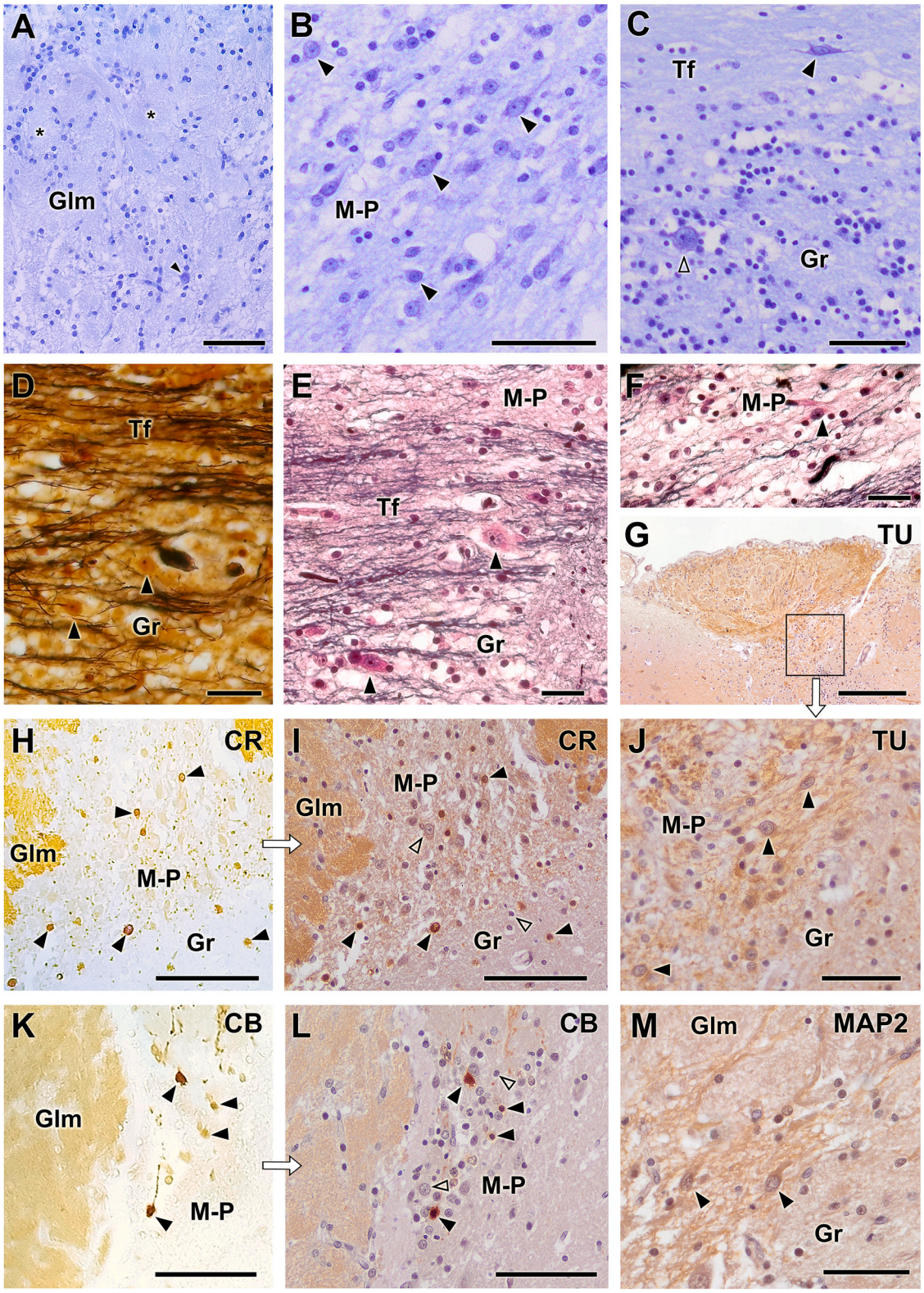

Fig. 3. Histological and immunohistochemical study of the fox AOB cytoarchitecture. A–C. Nissl stains of the accessory olfactory bulb (AOB) layers. A. Glomerular layer (Glm) showing some instances of the glomeruli (asterisk), whose boundaries are not neatly defined, and an isolated larger neuron in the deeper part (arrowhead). B. The principal cells of the AOB occupy a broad band that is designated as the mitral-plexiform (M-P) layer. The principal cells (arrowheads) display either miter or ellipsoid shapes and have large soma featuring large, rounded nuclei with patent nucleoli. Interspersed between the principal cells, numerous smaller cells containing round nuclei can be observed. C. A band of white matter corresponding to an axonal fiber tract (Tf) contains only large multipolar neurons (black arrowhead). Deeper to the Tf, the granular (Gr) layer is occupied by clusters of granular cells and isolated large neurons with oval soma (open arrowhead). D. Bielschowsky stain of the deep layers of the AOB showing the development of the Tf and its projections into the Gr layer, which consists of granule cells and larger, isolated neurons (arrowhead). E and F. Tolivia staining of the AOB, showing the Tf, arranged between the M-P and Gr layers. Scattered large neurons are interspersed among the myelinated fibers of the Tf (arrowhead) and the Gr layer (E). In the M-P layer, the principal cells (arrowhead) are intermingled with Tf projections (F). G and J. Sagittal sections of the AOB immunostained with anti-α-tubulin. An enlarged image of the M-P layer shows the α-tubulin-immunopositivity of mitral cell somas (arrowheads) and the surrounding neuropil. H and I. Immunostaining of the M-P layer with anti-calretinin. The left image shows the section

without counterstaining (H), whereas the right image shows the same section with hematoxylin counterstaining (I). Only a subpopulation of cells (black arrowheads) are calretinin-positive. K and L. Immunostaining of the M-P layer with anti-calbindin. The left image shows the section without counterstaining (K), whereas the right image shows the same section with hematoxylin counterstaining (L). A subpopulation of both large and small neuronal cells (black arrowheads) are calretinin-positive. Many cells remain unstained (open arrowheads). The immunolabeling pattern does not allow for the discrimination of a complementary neuronal distribution for these two markers, CB and CR. M. Immunostaining of the AOB with anti-MAP-2 results in the strong immunolabeling of mitral cell somas and their dendritic projections to the glomerular layer (arrowheads). Scale bars: A,H,I,K,L: 100 µm. B,C,J,M: 50 µm. D–F: 25 µm. G: 250 µm.

3.2.4. Comparative histological and immunohistochemical study of the dog and fox AOB

To illustrate the differences in lamination between the accessory olfactory bulb of the fox and the dog, we performed a comparative histological and immunohistochemical study of the dog and fox AOB, primarily focusing on the organization of the mitral-plexiform (M-P) layer, where the projection cells of the AOB are located. Tolivia staining (Fig. 8A) reveals less development of the M-P layer in the dog compared with the fox (Fig. 8B). The M-P layer in the dog consists of a thin layer with scattered principal cells, whereas, in the fox, the M-P layer neuropil projects into the glomerular layer (Glm), and its principal cells are numerous, with a typical mitral shape. Tolivia staining also reveals differences in the granular layer (Gr), which is mainly occupied by the lateral olfactory tract fibers in the dog, whereas, in the fox, these fibers are less dense, and more cellular elements can be observed. Nissl staining of the dog (Fig. 8C) and fox (Fig. 8D) AOB reveals differences in the thickness of the M-P layer and in the density of its principal cells, which are more numerous and have mitral shapes with clearly delineated somas in the fox AOB. Additionally, the granule cells in the fox AOB are organized into clusters, whereas, in the dog, they are scattered in a more diffuse pattern. Finally, immunohistochemical staining of the dog (Fig. 8E) and fox (Fig. 8F) AOB using anti-Gαo shows the characteristic shape and development of the M-P layer in each species.

4. Discussion

In canids, the current understanding of the first integrative center of the VNS, the AOB, is associated with a number of crucial and unresolved questions. The few existing studies of the canid AOB, limited to the dog, have indicated a small size and a lack of the typical cytoarchitecture observed in other mammalian species (Meisami and Bhatnagar, 1998). To better understand the relevance, in the context of the Canidae family, of the results presented here, it is therefore important to address the study of the AOB of the dog. A pioneering comparative study among the olfactory bulbs of carnivorous species performed by Jawlowski (1956) was the first to describe the AOB histology in dogs, which was succinctly described as "very small", and, additionally, remains, to our knowledge, as the only reference to the existence of an AOB in the fox. Although Jawlowski was unable to discern the presence of glomeruli in this putative fox AOB, his drawing of the structure at the caudomedial border of the MOB coincides with our macroscopic and microscopic observations. Years later, Miodonski (1968), in his description of the dog's olfactory bulb, characterized the dog AOB as a small-volume structure and poorly defined structure.

The contributions by Salazar et al. (1992, 1994) demonstrated for the first time the unequivocal linkage between this presumptive AOB and the VNOLater, Nakajima et al. (1998) divided the dog AOB into three layers: vomeronasal (Vn) and glomerular (Glm) layers, which occupied most of the AOB, and a thin neuronal cell layer containing several types of neurons. Most of these neurons featured round or oval soma and appeared to correspond with mitral/tufted cells. They only found a small number of granule cells, mainly in the inner portion of the neuronal cell layer, adjoining the olfactory peduncle.

4.1. Histological and immunohistochemical labeling of the fox AOB

Aiming to better comprehend the fox AOB, after the macroscopic identification of a presumptive AOB in an area similar to that described by Jawlowski, we performed a serial histological and immunohistochemical study that enabled the characterization of the

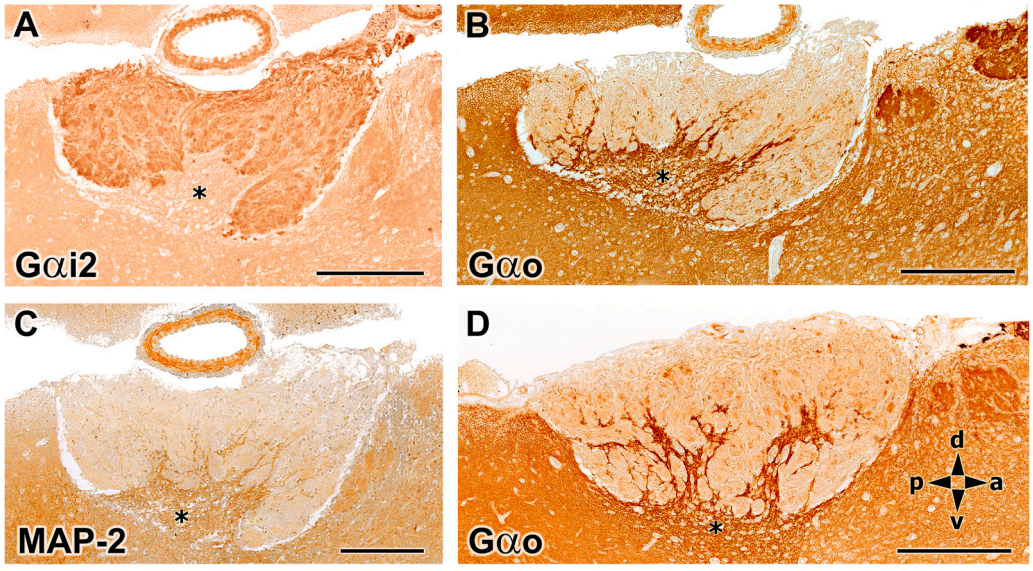

Fig. 4. Immunohistochemical labeling of the fox AOB. A. Immunopositive labeling of the AOB using the anti-Gαi2 antibody produced strong immunolabeling in the nervous and glomerular layers, whereas the immunolabeling in the mitral-plexiform layer was weaker. B and D. Anti-Gαo immunopositive labeling was observed in the same layers of the AOB in a complementary pattern to that observed for anti-Gαi2 labeling, with stronger immunostaining in the mitral-plexiform layer (asterisk) and weaker immunolabeling in both the vomeronasal nerve and glomerular layers; (B, younger fox; D, older fox). C. Anti-MAP-2 shows a similar pattern to anti-Gαo, in which the nervous and glomerular layers are immunonegative, and both the mitral-plexiform and granular layers are immunopositive (asterisk). The compass indicates the orientation, as follows: d, dorsal; v, ventral; p, posterior; a, anterior. Scale bars: 250 µm.

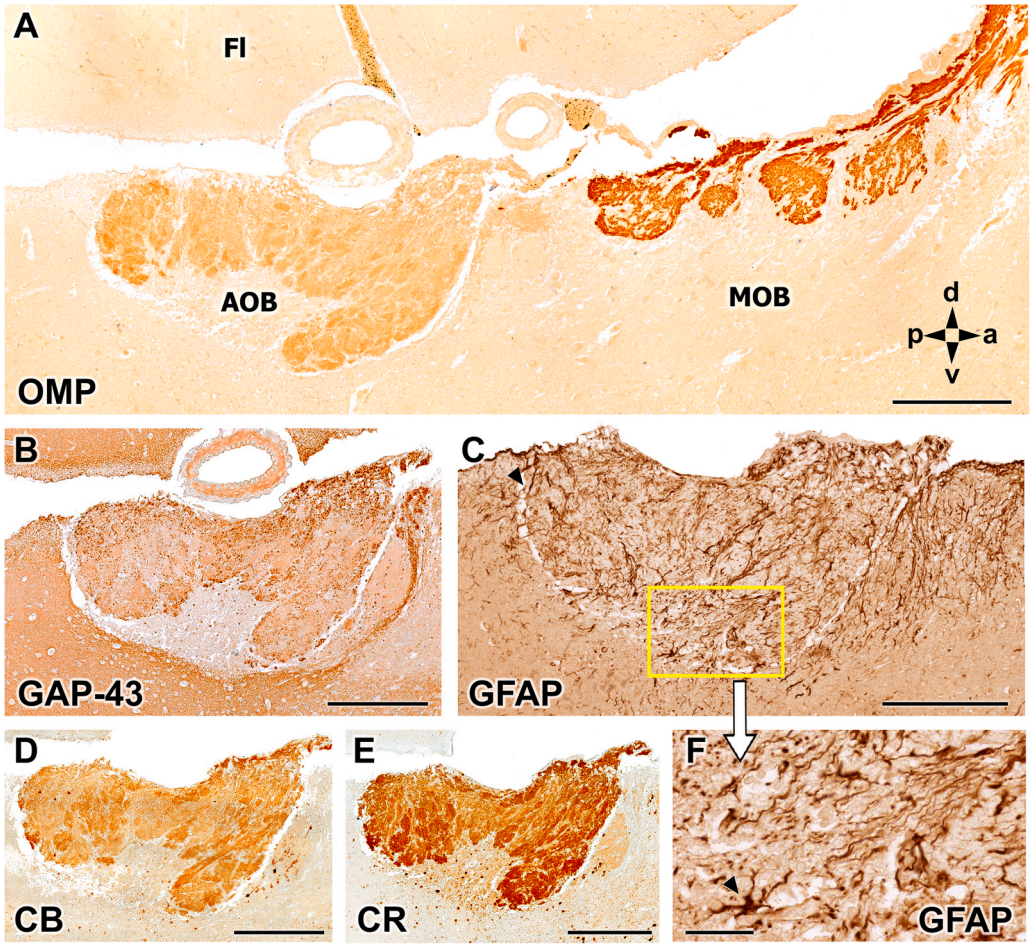

Fig. 5. Immunohistochemical labeling of the fox AOB. A. Immunopositive labeling in the vomeronasal nerve and glomerular layers with anti-olfactory marker protein (OMP). The main olfactory bulb (MOB) glomeruli are intensely labeled. B. Anti-growth-associated protein 43 (GAP-43) immunopositive labeling in the superficial layers of the accessory olfactory bulb (AOB). C. Anti-glial fibrillary acidic protein (GFAP) labels the dense arborizations of the ensheathing cells in both the vomeronasal and glomerular layers. Immunopositive astrocytes are observed in the deep layers (higher magnification of the yellow frame is shown in F, arrowhead). D and E. Similar immunopositive patterns as observed using anti-Gαi2 in the AOB were observed using anti-calbindin (CB) and anti-calreticulin (CR) antibodies (D and E, respectively). a, anterior; d, dorsal, p, posterior; v, ventral. Scale bars: A–E: 250 µm. F: 50 µm.

morphofunctional nature of the AOB. The main comparative structural findings are summarized in Fig. 9. Our observations of the microscopic texture of the fox AOB contrast with the available microscopic descriptions of the dog AOB. The most striking feature of the fox AOB is its clear lamination, with neatly differentiated layers, including a highly developed Glm layer, rich in periglomerular cells, and a large inner cell layer, equivalent to both the inner cell layer described by Salazar et al. (1992, 1994) and the neuronal cell layer described by Nakajima et al. (1998) but more easily discernible. Unlike in the dog AOB, this layer is not a thin sheet in the fox but instead appears as a large area projecting inward onto the superficial layers of the AOB. This observation was especially apparent following the immunohistochemical staining, which was able to clearly differentiate the two outer layers, the Vn and Glm layers, from the inner cellular zone. The inner layer was immunonegative when using antibodies against Gαi2, OMP, and GAP-43, whereas the two outer layers were immunopositive. By contrast, immunopositive labeling was observed using the anti-Gαo and anti-MAP-2 antibodies in the inner layers, but the outer layers were immunonegative. The strong labeling obtained in the two superficial layers against OMP, which is a marker for mature vomeronasal cells (Bock et al., 2009), and against GAP-43, one of the best-characterized markers for growing and regenerating neuronal processes (Ramakers et al., 1992), indicates important activity in the fox VNS among both mature and regenerating vomeronasal neurons. Anti-CB and anti-CR staining also produced intense labeling in the Vn and Glm layers, which is consistent with the expression found in the fox VNO, both in the neuroepithelium and in the NVN of the lamina propria. Although the expression of these markers has been observed in subpopulations of neuroreceptor cells (Ortiz-Leal et al., 2020), at the level of the AOB, these neurons do not show topographic segregation, integrating their axons throughout the anteroposterior axis of the AOB. The high density of cell bodies and fibers stained with anti-GFAP in the Vn layer, encompassing glomeruli, and in the M-P layer of the fox AOB contrasts with the scarce number of astrocytes found in the dog AOB (Fig. 8 in Salazar et al., 1994), and is reminiscent of the profuse labeling observed in the rat olfactory bulb (Bailey and Shipley, 1993). This high level of GFAP expression in the fox AOB suggests a very active neuron-glial interaction, which is known to be involved in various processes in adults, such as synaptic communication, plasticity, homeostasis, and dynamic monitoring and alteration of the central nervous system structure and function (Allen and Lyons, 2018).

MAP-2 expression is particularly relevant because it can be used to identify AOB principal cell somas and dendritic trees (Dehmelt and Halpain, 2005; Villamayor et al., 2020). In contrast to the scarce number of mitral cells described in previous studies of the dog AOB, numerous mitral cells were observed in the fox AOB, distributed in parallel along a broad band and displaying either miter or ellipsoid shapes. We designated this layer as the M-P layer, and antibodies

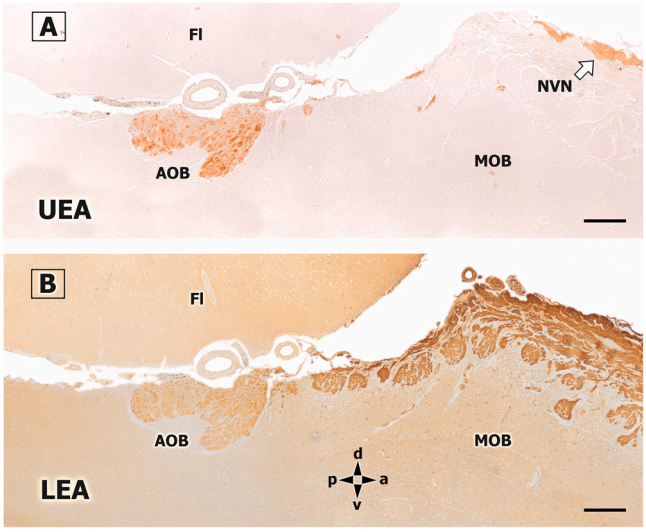

Fig. 6. Lectin-histochemical study of the fox AOB and MOB. A. Ulex europeus agglutinin I (UEA-I) labels the superficial layers of the accessory olfactory bulb (AOB; nervous and glomerular layers) and the branches of the vomeronasal nerves (NVN). However, the olfactory nerve layer and the glomeruli of the main olfactory bulb (MOB) are not labeled with UEA. B. Lycopersicon esculentum agglutinin (LEA) stains the superficial layers in both the AOB and the MOB. Fl, frontal lobe of the telencephalon. The compass indicates the orientation, as follows: d, dorsal; v, ventral; p, posterior; a, anterior. Scale bars: 250 µm.

against both MAP-2 and α-tubulin allowed for the discrimination of these cells and their dendrites. Mitral cells serve as the main projection neurons of the AOB, and their high density is also reflected by the development of the Tf that they form and that could be observed using Tolivia and Bielschowsky staining. These fibers represent the contribution of the AOB to the dorsal portion of the LOT, which runs below the inner granular cells in the fox, coinciding with the observation reported by Switzer et al. (1980) in their extensive comparative study of the mammalian LOT.

Overall, a high degree of development was observed for the mitral cells in the fox AOB, which were very abundant and presented with varied morphologies, and for the plexiform layer, in which the dendritic trees of the mitral cells are distributed, which was particularly striking compared with the low numbers of mitral cells and the scarce plexiform layer development described in the dog AOB by Salazar et al. (1994) and Nakajima et al. (1998). For example, Fig. 3B in the results section shows the cellular organization of the mitral-plexiform layer of the fox AOB, which is similar to the M-P layer observed in the AOB of species with maximal VNS development, such as the rat (Larriva-Sahd, 2008) or the rabbit (Villamayor et al., 2020). In the granular zone, both Tolivia and Bielschowsky stainings allowed for the discrimination of an extensive granular cell presence, which formed clusters between the Tf and the LOT. In both the granular and the M-P layer, anti-CB and anti-CR staining allowed for the discrimination of neuronal subpopulations. However, we cannot compare the fox with the dog because anti-CR and anti-CB antibodies have not been used in dogs, although the pattern observed in the fox is comparable to that observed in the mouse and the rabbit (Jia and Halpern, 2004; Villamayor et al., 2020).

4.2. Lectin-histochemical labeling of the fox AOB

Our recent study of the fox VNO allowed us to determine the validity of using the lectins UEA-I and LEA as VNO receptor markers in the neuroepithelium (Ortiz-Leal et al., 2020). By extending this study of the fox VNS to the NVN and the AOB, we have determined that LEA stains the NVN and the superficial nervous and glomerular elements of both the AOB and MOB, whereas UEA-I specifically

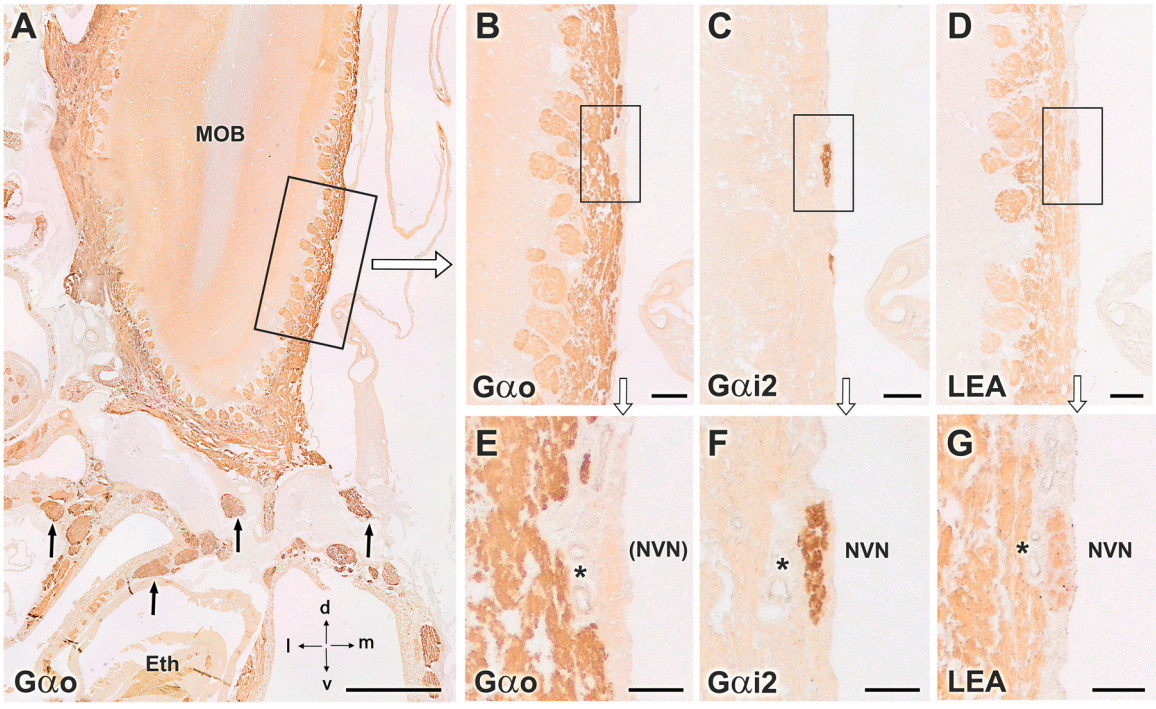

Fig. 7. Immunohistochemical and lectin-histochemical study of the vomeronasal nerve (NVN) in the ethmoidal fossa (Eth). Serial sections of the main olfactory bulb (MOB) in the ethmoidal fossa were stained with anti-G o (A, B, and E), anti-Gαi2 (C and F), and the lectin LEA (D and G). A. Anti-Gαo stained the olfactory nerves in the ethmoidal concha (arrows) and the superficial layers, both nervous and glomerular, of the MOB. B. The trajectory of the NVN along the ventromedial surface of the MOB is not labeled with this marker. C. Anti-Gαi2 only stains the NVN. D. The lectin LEA labels both the olfactory nerve layer of the MOB and the NVN. E–G. A higher magnification image of the NVN using the same markers confirmed that the NVN is Gαo-immunonegative and Gαi2–immunopositive. The presence of small arterioles (asterisk) in a plane deep to the NVN serves as a useful landmark for locating the unstained nerve in E. d, dorsal; l, lateral; m, medial; v, ventral. Scale bars: A: 1 mm. B–D: 100 µm. E–G: 50 µm.

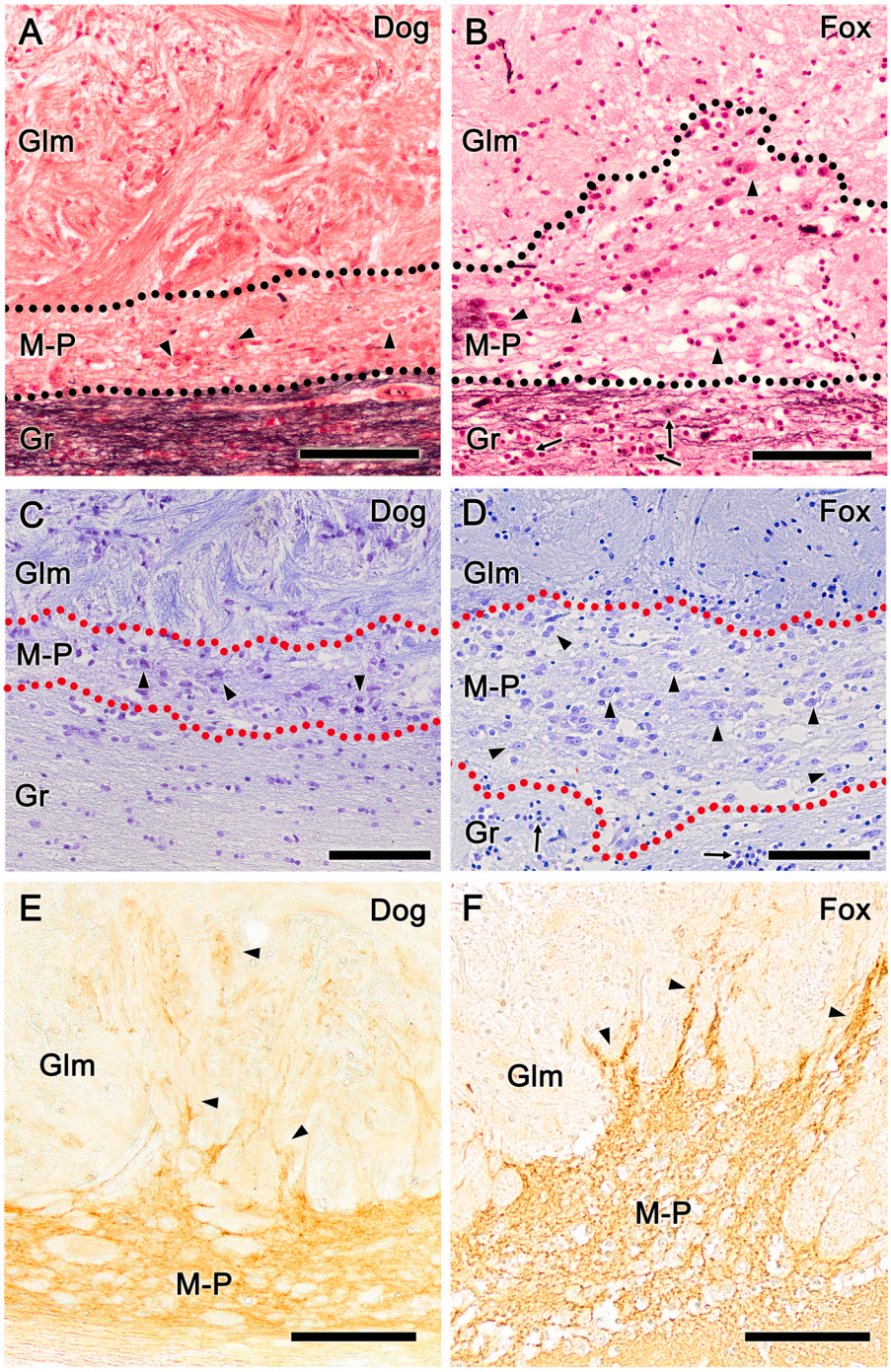

Fig. 8. Comparative histological and immunohistochemical study of the dog and fox AOB. A and B. Tolivia staining of the dog (A) and fox (B) AOB showing the reduced development of the mitral-plexiform layer (M-P) in dogs. The M-P layer in the dog consists of a thin layer with scattered principal cells, whereas, in the fox, the M-P layer neuropil projects into the glomerular layer (Glm), and the principal cells are more numerous and have a typical mitral shape. The granular layer (Gr) is primarily occupied by lateral olfactory tract fibers in dogs. These fibers are less dense in the fox AOB. C and D. Nissl staining of the dog (C) and fox (D) AOB. Both images are at the same magnification. The differences in the thickness of the M-P layer and in the principal cell density (arrowheads) are appreciable. The principal cells of the fox AOB are more numerous and have mitral shapes with clearly delineated somas. The granule cells in the fox AOB are organized into clusters (arrows), whereas, in the dog, they are scattered. E and F. Immunohistochemical staining of the dog (E) and fox (F) AOB with anti-Gαo, which shows the characteristic shape and development of the M-P layer in each species. Scale bars: 100 µm.

stains only the NVN and the AOB. This finding demonstrates the usefulness of UEA-I as a specific marker of the fox vomeronasal pathway and is identical to the finding obtained in the dog, in which a similar VNS-specific pattern was obtained using UEA-I staining (Salazar et al., 1994).

This result is even more significant if we consider that the UEA-I labeling pattern in the VNS varies greatly across different types of mammals. UEA-I has also been demonstrated to serve as a specific marker of the vomeronasal pathway (VNO, NVN, and AOB) in adult mice (Kondoh et al., 2017; Salazar et al., 2001) but does not label the AOB in the rabbit (Villamayor et al., 2020), sheep (Salazar et al., 2000) and roe deer (Park et al., 2014). In other species, including rats (Salazar and Sánchez Quinteiro, 1998), capybaras (Torres et al., 2020), and pigs (Salazar et al., 2000), UEA-I labels both the MOS and the VNS.

The labeling pattern observed for LEA in the fox coincides with that described for the dog (Salazar et al., 2013), serving as a general

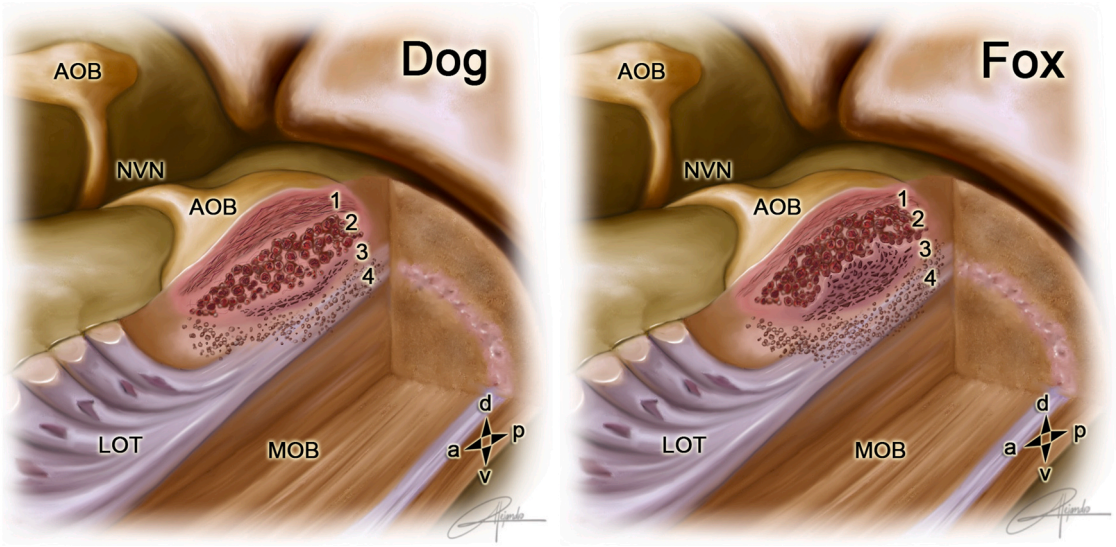

Fig. 9. Drawings of the dog (A) and fox (B) olfactory bulbs, showing the typical lamination of the accessory olfactory bulb in each species. AOB, accessory olfactory bulb; MOB, main olfactory bulb; LOT, lateral olfactory tract; 1, Vomeronasal nerve layer; 2, Glomerular layer; 3, Mitral-plexiform layer; 4, Granular layer. Compass points indicate the orientation: d, dorsal; p, posterior; v, ventral; a, anterior.

marker for both the MOB and AOB. This LEA labeling pattern is common across a wide range of studied species, as diverse as mice, sheep, pigs, deer, rabbits, and capybaras (Salazar et al., 2000 and 2001; Park et al., 2014; Villamayor et al., 2020, Torres et al., 2020). Overall, these findings demonstrate that the pattern of glycoconjugate expression detected by both lectins (L-fucose for UEA-I and N-acetyl-β-D-glucosamine for LEA) is highly conserved in the canid VNS.

4.3. G-protein immunohistochemistry in the fox AOB

Recent findings have demonstrated immunopositivity against the G-protein subunits Gαi2 and Gαo in both the neuroreceptor epithelium and the vomeronasal axons of the parenchyma in the fox VNO (Ortiz-Leal et al., 2020), which represents an important difference from the observations in the dog VNO. In dogs, Gαo protein expression has not been detected (Salazar et al., 2013), except for the study reported by Dennis et al. (2003), in which the authors expressed doubts regarding the labeling validity due to the use of antigenic retrieval. Gαo positivity would imply the effective expression of V2R receptors in the dog VNO, contradicting the inability to identify functional V2R family genes in either the dog (Young and Trask, 2007) or fox genome (Kukekova et al., 2018).

To explore the role played by Gαo neuroreceptor cells in the fox VNS, we first investigated Gαo expression in the fox AOB. Anti-Gαo immunolabeling was negative in the superficial layers of the AOB, suggesting that the vomeronasal axons that project to the AOB are Gαo-negative. Although the internal layers of the AOB are Gαo-positive, this finding is common to all mammalian species, as the entire olfactory bulb, including both the AOB and MOB, is Gαo-immunopositive, except for the Vn and Glm layers of the AOB which correspond to the projections of V1R neuroreceptor cells, which are Gαi2-positive. These findings suggest that the Gαo axons that arise from the VNO do not project to the AOB. Regrettably, once these axons leave the VNO and integrate into the nasal submucosa, they become impossible to differentiate from olfactory nerves because Gαo is ubiquitously expressed on both olfactory and vomeronasal axons throughout the nasal mucosa lamina propria (Wekesa and Anholt, 1999).

To better understand the fates of these axons, we performed an immunohistochemical and lectin study in decalcified transverse sections of the ethmoidal fossa at a level rostral to the AOB, which included both the olfactory and vomeronasal axons on the surface of the MOB and in the ethmoidal turbinates. At this level, the vomeronasal axons have already coalesced into an NVN trunk that can be visualized using lectin and G-protein immunolabeling. Given the specific vomeronasal character of Gαi2 labeling, Gαi2 could be used to clearly differentiate the trajectories of NVNs. Serial consecutive sections demonstrated that these axons were Gαo-immunonegative and LEA-positive, with LEA serving as a universal marker of both olfactory systems. These results, therefore, indicate that the fox Gαo vomeronasal axons follow a fate leading to the olfactory bulb that occurs independently from NVNs, possibly converging with the axons of olfactory nerves to project to MOB glomeruli.

Until the identity of the receptors associated with the fox VNO Gαo-immunopositive neurons is established, the true character of these receptors, either vomeronasal or olfactory, cannot be determined. However, electrophysiological studies in mice have shown that a subpopulation of vomeronasal neurons has the ability to perceive odorants (Sam et al., 2001; Trinh and Storm, 2003), and more recent transcriptomic studies, such as that by Ibarra-Soria et al. (2014) in mice, have demonstrated the expression of ORs in the VNO. A total of 17 OR genes were expressed in the VNO at levels greater than the median expression level of vomeronasal receptor genes. Therefore, our finding that the fox VNO Gαo-positive neuroreceptor cells do not project to the AOB could support the presence of a direct pathway from the VNO to the MOB, suggesting the involvement of higher cortical areas in VNO-mediated odor perception and discrimination.

The possibility that specific information processing arising from Gαo neurons of the VNO could occur at the level of specific olfactory bulb structures should not be discounted, comparable to previously identified atypical glomeruli in rodents (Zimmerman and Munger, 2021) or the sub-bulbar accessory nuclei of the rabbit (Villamayor et al., 2020). Although no structures of this nature have yet been identified in any canid olfactory bulb, our own observations in the fox olfactory bulb indicate the potential presence of these atypical structures, where information from the VNO may be processed.

4.4. Can domestication shape Canidae accessory olfactory bulb morphology?

A long-term experiment designed to reproduce early mammalian domestication in the silver fox makes this species a particularly

useful model for studying the effects of domestication in Canidae (Belyaev et al., 1985; Wang et al., 2018). The selection of fox for tameability or amenability to domestication led to changes in behavior, physiology, and genetic diversity, similar to those observed in domestic dogs (Trut el al, 2009, Kukekova et al., 2018). Domestication has also led to striking anatomical changes, whose nature and sources of variation are intriguing. In the nervous system, domestication is known to affect developmental neurotransmitter systems (Popova, 2006); however, the neuromorphological changes that occur following the selection for tameness in the Russian fox-farm experiment have only recently been explored in a comprehensive manner. As a result, a change in gray matter volume was observed in tame strains relative to conventional farm foxes, which suggested that selection for behavior can influence brain morphology (Hecht et al., 2021).

These findings present the possibility that the striking structural differences observed between the dog and the fox AOB may partially be the result of the domestication process. To our knowledge, this would represent the first evidence that domestication and concerted artificial selection act to shape the neuroanatomical basis of the accessory olfactory system. The observed variations are unlikely to be attributable to interspecies differences, as no examples exist among mammals belonging to the same family that display such remarkable divergences in the configurations of the VNO and AOB. Even among bats, which have been characterized as having great morphological diversity in the VNS among different families, the pattern observed within each family is highly conserved (Baron et al., 1996). However, we cannot exclude the possibility that other causes may underlie the observed anatomical differences between the AOBs of the fox and the dog. One possibility is the differential evolution of the vomeronasal system between these two species due to adaptations to the different lifestyles typical of the wild fox and the dog. The size of the vomeronasal type 1 receptor (V1R) gene repertoire is known to be a good indicator of the relationship between animal genomes and their environmental niche specializations, especially the relationship between ecological factors and the molecular evolutionary history of the sensory system (Wang et al., 2010). Domestication is also known to affect variations in gene expression patterns throughout the genome, with domesticated species generally exhibiting lower gene expression diversity than wild species (Liu et al., 2019). Therefore, one potential avenue for the further investigation of morphofunctional differences between the AOBs of the fox and the dog would be a comparative transcriptomic analysis using RNA-seq on AOB samples from both species. Epigenetic studies of AOB samples would also be informative, as methylation profiles have indicated that epigenetic factors were involved in the speciation process from wild canids to the domestic dog (Sundman et al., 2020).

Given that the dog was originally domesticated from the wolf, a future step of our study will include the performance of morphofunctional studies on the accessory olfactory system of the wolf, for which no references are currently available. The divergence of the dog from the wolf is thought to have occurred approximately 12,000–15,000 years ago (Graphodatsky et al., 2008), which is a relatively short time span on the evolutionary scale. Therefore, further structural and genomic studies of the wolf AOB could contribute to a better understanding of the nature and sources of variation that occur under domestication pressure.

The anatomical differences encountered support the current hypothesis that the domestication of the dog has resulted in an involution of olfactory development associated with the detection of pheromones and other semiochemicals by the accessory olfactory system (Jezierski et al., 2016). Recent evidence suggests that the loss of olfactory capacity in dogs is a result of domestication-related changes in the MOS, which serves as a morphological comparison. Specifically, Deborah Bird and Blaire Van Valkenburg examined cribriform plate (CP) morphology in 46 dog breeds and 2 wild canids, the coyote and gray wolf, using high-resolution computed tomography scans and digital quantification, which revealed that dogs, even among those breeds with well-recognized olfactory capabilities, have reduced CP surface areas relative to body size compared with both the wolf and coyote (Bird et al., 2021). Previously, these authors studied all mammalian superorders and demonstrated that relative CP size is closely correlated with the number of OR genes in a species' genome, establishing CP size as a metric for evolutionary expansions or losses in the mammalian olfactory systems (Bird et al., 2018). These differences could further be examined to determine the comparative morphological changes in the MOB of wild and domestic canids.

Finally, whether similar changes as those found in the dog can be observed in other domesticated mammals, such as the cat, remains to be determined. However, cats have a shorter domestication period than dogs; dogs are estimated to have been domesticated approximately 33,500 years ago (Perri, 2016), whereas the earliest evidence of domestic cats dates to approximately 9500 years ago in Cyprus and approximately 5000 years ago in central China (Vigne et al., 2004; Hu et al., 2014). Cats and humans were thought to interact throughout this period in a commensal manner, in which tamed and domestic cats intermixed with wild subspecies, which could account for the reduced differentiation observed between wild and domestic cat genomes (Montague et al., 2014). Furthermore, the morphological, physiological, behavioral, and ecological traits of cats do not appear to have been greatly affected by the domestication process (Zeder, 2012), in contrast with observations made for the dog (Axelsson et al., 2013). Currently, no studies are available examining the AOB of wild cats, making it impossible to assess whether morphofunctional changes can be observed between the AOBs of wild and domestic cats.

In summary, in this study, we morphofunctionally characterized the fox AOB, providing useful information toward understanding the VNS of wild canids. This in-depth, histological, immunohistochemical, and lectin-histochemical study demonstrated that the fox AOB presents unique characteristics and a higher degree of morphological development compared with the dog AOB. These morphofunctional findings suggest that a decrease in the anatomical complexity of the accessory olfactory system occurred at some point during the evolutionary history of dogs and opens a new research avenue for studying the effects of domestication on brain structures.

Acknowledgments

Special thanks are due to Alejandro García MD, DVM for his artistic drawings of the AOB topography. The red foxes used in this study were provided by the Wildlife Recovery Centres of Galicia, Dirección Xeral de Patrimonio Natural (Xunta de Galicia, Spain) and by Federación Galega de Caza.

Author contributions

P.S.Q. and I.O.L. designed the research and wrote the paper. P.S.Q., I.O.L., and M.T. performed the work, and P.S.Q., I.O.L., M.T., P.V., L-E.F. and A.L.B performed analyzed and discussed the results.

Conflict of interest

The authors declare that the research was conducted in the absence of any commercial or financial relationships that could be construed as a potential conflict of interest.

Ethical approval

All the animals employed in this study dead by natural causes.

Funding

This work was supported by a University of Santiago de Compostela, Spain, grant [1551-8179] to P.S.Q.

References

Adrio, F., Rodríguez-Moldes, I., Anadón, R., 2011. Distribution of glycine immunoreactivity in the brain of the Siberian sturgeon (*Acipenser baeri*): comparison with γ-aminobutyric acid. J. Comp. Neurol. 519, 1115–1142. https://doi.org/10.1002/cne.22556

Allen, N.J., Lyons, D.A., 2018. Glia as architects of central nervous system formation and function. Science 362, 181–185. https://doi.org/10.1126/science.aat0473

Axelsson, E., Ratnakumar, A., Arendt, M.L., Maqbool, K., Webster, M.T., Perloski, M., Liberg, O., Arnemo, J.M., Hedhammar, A., Lindblad-Toh, K., 2013. The genomic signature of dog domestication reveals adaptation to a starch-rich diet. Nature 495, 360–364. https://doi.org/10.1038/nature11837

Bailey, M.S., Shipley, M.T., 1993. Astrocyte subtypes in the rat olfactory bulb: morphological heterogeneity and differential laminar distribution. J. Comp. Neurol. 28, 501–526. https://doi.org/10.1002/cne.903280405

Baron, G., Stephan, H., Frahm, H.D., 1996. Comparative neurobiology in Chiroptera. Vols. 1, 2, and 3. Burkhauser Verlag, Berlin.

Barrios, A.W., Núñez, G., Sánchez Quinteiro, P., Salazar, I., 2014. Anatomy, histochemistry, and immunohistochemistry of the olfactory subsystems in mice. Front. Neuroanat. 8, 63. https://doi.org/10.3389/fnana.2014.00063

Belyaev, D.K., Plyusnina, I.Z., Trut, L.N., 1985. Domestication in the silver fox (*Vulpes fulvus* Desm): changes in physiological boundaries of the sensitive period of primary socialization. Appl. Anim. Behav. Sci. 13, 359–370. https://doi.org/10.1016/0168-1591(85)90015-2

Berghard, A., Buck, L.B., 1996. Sensory transduction in vomeronasal neurons: evidence for G alpha o, G alpha i2, and adenylyl cyclase II as major components of a pheromone signaling cascade. J. Neurosci. 16, 909–918. https://doi.org/10.1523/JNEUROSCI.16-03-00909.1996

Bird, D.J., Jacquemetton, C., Buelow, S.A., Evans, A.W., Van Valkenburgh, B., 2021. Domesticating olfaction: Dog breeds, including scent hounds, have reduced cribriform plate morphology relative to wolves. Anat. Rec. 304, 139–153. https://doi.org/10.1002/ar.24518

Bird, D.J., Murphy, W.J., Fox-Rosales, L., Hamid, I., Eagle, R.A., Van Valkenburgh, B., 2018. Olfaction written in bone: cribriform plate size parallels olfactory receptor gene repertoires in Mammalia. Proc. Biol. Sci. 285, 20180100. https://doi.org/10.1098/rspb.2018.0100

Bock, P., Rohn, K., Beineke, A., Baumgärtner, W., Wewetzer, K., 2009. Site-specific population dynamics and variable olfactory marker protein expression in the postnatal canine olfactory epithelium. J. Anat. 215, 522–535. https://doi.org/10.1111/j.1469-7580.2009.01147.x

Cajal, S.R., 1902. Textura del lóbulo olfativo accesorio. Rev. Micros. 1, 141–150.

Clancy, A.N., Coquelin, A., Macrides, F., Gorski, R.A., Noble, E.P., 1984. Sexual behavior and aggression in male mice: involvement of the vomeronasal system. J. Neurosci. 4, 2222–2929. https://doi.org/10.1523/JNEUROSCI.04-09-02222.1984

Coppola, J., Disney, A., 2018. Most calbindin-immunoreactive neurons, but few calretinin-immunoreactive neurons, express the m1 acetylcholine receptor in the middle temporal visual area of the macaque monkey. Brain Behav. 8, e01071 https://doi:10.1002/brb3.1071.

De Góis Morais, P.L.A., Paiva, K.M., Oliveira, R.F., Santana, M.A.D., Guzen, F.P., Engelberth, R.C.G.J., de Souza Cavalcante, J., Nascimento, E.S., Cavalcanti, J.R.L.P., 2021. Distribution and morphology of calbindin neurons in the Amygdaloid Complex of the marmoset monkey (*Callithrix jacchus*). J. Chem. Neuroanat. 112, 101914 https://doi:10.1016/j.jchemneu.2020.101914.

De la Rosa-Prieto, C., Saiz-Sanchez, D, Ubeda-Bañon, I., Argandoña-Palacios, L., Garcia-Muñozguren, S., Martinez-Marcos, A., 2010. Neurogenesis in subclasses of vomeronasal sensory neurons in adult mice. Dev. Neurobiol. 70, 961–970 https://doi: 10.1002/dneu.20838.

Dehmelt, L., Halpain, S., 2005. The MAP2/Tau family of microtubule-associated proteins. Genome Biol. 6, 204. https://doi.org/10.1186/gb-2004-6-1-204

Del Cerro, M.C., 1998. Role of the vomeronasal input in maternal behavior. Psychoneuroendocrinology 23, 905–926. https://doi.org/10.1016/s0306-4530(98)00060-2

Dennis, J.C., Allgier, J.G., Desouza, L.S., Eward, W.C., Morrison, E.E., 2003. Immunohistochemistry of the canine vomeronasal organ. J. Anat. 202, 515–524. https://doi.org/10.1046/j.1469-7580.2003.00190.x

Frahm, H.D., Bhatnagar, K.P., 1980. Comparative morphology of the accessory olfactory bulb in bats. J. Anat. 130, 349–365.

Gonzalez-Lozano, M.A., Klemmer, P., Gebuis, T., Hassan, C., van Nierop, P., van Kesteren, R.E., Smit, A.B., Li, K.W., 2016. Dynamics of the mouse brain cortical synaptic proteome during postnatal brain development. Sci. Rep. 6, 35456. https://doi.org/10.1038/srep35456

Graphodatsky, A.S., Perelman, P.L., Sokolovskaya, N.V., Beklemisheva, V.R., Serdukova, N.A., Dobigny, G., O'Brien, S.J., Ferguson-Smith, M.A., Yang, F., 2008. Phylogenomics of the dog and fox family (Canidae, Carnivora) revealed by chromosome painting. Chromosome Res. 16, 129–143. https://doi.org/10.1007/s10577-007-1203-5

Gutiérrez-Castellanos, N., Pardo-Bellver, C., Martínez-García, F., Lanuza, E., 2014. The vomeronasal cortex – afferent and efferent projections of the posteromedial cortical nucleus of the amygdala in mice. Eur. J. Neurosci. 39, 141–158. https://doi.org/10.1111/ejn.12393

Halpern, M., 1987. The organization and function of the vomeronasal system. Ann. Rev. Neurosci. 10, 325–362. https://doi.org/10.1146/annurev.ne.10.030187.001545

Halpern, M., Martínez-Marcos, A., 2003. Structure and function of the vomeronasal system: an update. Prog. Neurobiol. 70, 245–318. https://doi.org/10.1016/s0301-0082(03)00103-5

Hecht, E.E., Kukekova, A.V., Gutman, D.A., Acland, G.M., Preuss, T.M., Trut, L.N., 2021. Neuromorphological changes following selection for tameness and aggression in the Russian fox-farm experiment. J. Neurosci. 41, 6144–6156. https://doi.org/10.1523/JNEUROSCI.3114-20.2021. (Advance online publication).

Hermanowicz-Sobieraj, B., Bogus-Nowakowska, K., Robak, A., 2018. Calcium-binding proteins expression in the septum and cingulate cortex of the adult guinea pig. Ann. Anat. 215, 30–39 https://doi: 10.1016/j.aanat.2017.09.009.

Herrada, G., Dulac, C., 1997. A novel family of putative pheromone receptors in mammals with a topographically organized and sexually dimorphic distribution. Cell 90, 763–773. https://doi.org/10.1016/s0092-8674(00)80536-x

Holy, T.E., 2018. the accessory olfactory system: innately specialized or microcosm of mammalian circuitry? Ann. Rev. Neurosci. 41, 501–525. https://doi.org/10.1146/annurev-neuro-080317-061916

Hu, Y., Hu, S., Wang, W., Wu, X., Marshall, F.B., Chen, X., Hou, L., Wang, C., 2014. Earliest evidence for commensal processes of cat domestication. Proc. Nat. Acad. Sci. USA 111, 116–120. https://doi.org/10.1073/pnas.1311439110

Ibarra-Soria, X., Levitin, M.O., Saraiva, L.R., Logan, D.W., 2014. The olfactory transcriptomes of mice. PLoS Genet. 10, e1004593. https://doi.org/10.1371/journal.pgen.1004593

Ichikawa, M., Osada, T., Ikai, A., 1992. Bandeiraea simplicifolia lectin I and Vicia villosa agglutinin bind specifically to the vomeronasal axons in the accessory olfactory bulb of the rat. Neurosci. Res. 13, 73–79. https://doi.org/10.1016/0168-0102(92)90035-b

Jawlowski, H., 1956. On the bulbus olfactorius and bulbus olfactorius accessorius of some mammals. Lub. Uniw. Marii Curie-Sklodowskiej Rocz. Annls. Dzialc. Nauk. Biol. 10, 67–86.

Jezierski, T., Ensminger, J., Papet, L.E., 2016. Canine Olfaction Science and Law: Advances in Forensic Science, Medicine, Conservation, and Environmental Remediation. CRC Press/Taylor & Francis, Boca Ratón, FL.

Jia, C., Halpern, M., 2004. Calbindin D28k, parvalbumin, and calretinin immunoreactivity in the main and accessory olfactory bulbs of the gray short-tailed opossum, Monodelphis domestica. J. Morphol. 259, 271–280. https://doi.org/10.1002/jmor.10166

Kaminski, J., Marshall-Pescini, S., 2014. The Social Dog: Behaviour and Cognition. Academic Press.

Kondoh, D., Kamikawa, A., Sasaki, M., Kitamura, N., 2017. Localization of α1-2 fucose glycan in the mouse olfactory pathway. Cells Tiss. Org. 203, 20–28. https://doi.org/10.1159/000447009

Koo, J.H., Saraswati, M., Margolis, F.L., 2005. Immunolocalization of Bex protein in the mouse brain and olfactory system. J. Comp. Neurol. 487, 1–14 https://doi: 10.1002/cne.20486.

Kotani, T., Murata, Y., Ohnishi, H., Mori, M., Kusakari, S., Saito, Y., Okazawa, H., Bixby, J.L., Matozaki, T., 2010. Expression of PTPRO in the interneurons of adult mouse olfactory bulb. J. Comp. Neurol. 518, 119–136 https://doi: 10.1002/cne.22239.

Kukekova, A.V., Johnson, J.L., Xiang, X., Feng, S., Liu, S., Rando, H.M., Kharlamova, A.V., Herbeck, Y., Serdyukova, N.A., Xiong, Z., Beklemischeva, V., Koepfli, K.P., Gulevich, R.G., Vladimirova, A.V., Hekman, J.P., Perelman, P.L., Graphodatsky, A.S., O'Brien, S.J., Wang, X., Clark, A.G., Zhang, G., 2018. Red fox genome assembly identifies genomic regions associated with tame and aggressive behaviours. Nat. Ecol. Evol. 2, 1479–1491. https://doi.org/10.1038/s41559-018-0611-6

Kukekova, A.V., Trut, L.N., Acland, G.M., 2014. Genetics of domesticated behavior in dogs and cfoxes. In: Grandin, T., Deesing, M.J. (Eds.), Genetics and the Behavior of Domestic Animals. Cambridge Academic Press.

Larriva-Sahd, J., 2008. The accessory olfactory bulb in the adult rat: a cytological study of its cell types, neuropil, neuronal modules, and interactions with the main olfactory system. J. Comp. Neurol. 510, 309–350. https://doi.org/10.1002/cne.21790

Liu, W., Chen, L., Zhang, S., Hu, F., Wang, Z., Lyu, J., Wang, B., Xiang, H., Zhao, R., Tian, Z., Ge, S., Wang, W., 2019. Decrease of gene expression diversity during domestication of animals and plants. BMC Evol. Biol. 19, 19. https://doi.org/10.1186/s12862-018-1340-9

Martínez-Ricós, J., Agustín-Pavón, C., Lanuza, E., Martínez-García, F., 2008. Role of the vomeronasal system in intersexual attraction in female mice. Neuroscience 153, 383–395. https://doi.org/10.1016/j.neuroscience.2008.02.002

Matsunami, H., Buck, L.B., 1997. A multigene family encoding a diverse array of putative pheromone receptors in mammals. Cell 90, 775–784. https://doi.org/10.1016/s0092-8674(00)80537-1

McLean, S., Nichols, D.S., Davies, N.W., 2021. Volatile scent chemicals in the urine of the red fox, Vulpes vulpes. PLoS One 16, e0248961. https://doi.org/10.1371/journal.pone.0248961

Meisami, E., Bhatnagar, K.P., 1998. Structure and diversity in mammalian accessory olfactory bulb. Microsc. Res. Tech. 43, 476–499. https://doi.org/10.1002/(SICI)1097-0029(19981215)43:6<476::AID-JEMT2>3.0.CO;2-V

Miodonski, R., 1968. Bulbus olfactorius of the dog (Canis familiaris). Acta Biol. Crac. 11, 65–75.

Montague, M.J., Li, G., Gandolfi, B., Khan, R., Aken, B.L., Searle, S.M., Minx, P., Hillier, L.W., Koboldt, D.C., Davis, B.W., Driscoll, C.A., Barr, C.S., Blackistone, K., Quilez, J., Lorente-Galdos, B., Marques-Bonet, T., Alkan, C., Thomas, G.W., Hahn, M.W., Menotti-Raymond, M., O'Brien, S.J., Wilson, R.K., Lyons, L.A., Murphy, W.J., Warren, W.C., 2014. Comparative analysis of the domestic cat genome reveals genetic signatures underlying feline biology and domestication. Proc. Nat. Acad. Sci. USA 111, 17230–17235. https://doi.org/10.1073/pnas.1410083111

Nakajima, T., Sakaue, M., Kato, M., Saito, S., Ogawa, K., Taniguchi, K., 1998. Immunohistochemical and enzyme-histochemical study on the accessory olfactory bulb of the dog. Anat. Rec. 252, 393–402. https://doi.org/10.1002/(SICI)1097-0185(199811)252:3<393::AID-AR7>3.0.CO;2-T

Nawaz, S., Akkaya, Özden, Dikmen, Ö., Altunbaş, T., Yağci, K., Kibria, A., Erdoğan, A.S.M.G., Çelik, H.A, M., 2020. Molecular characterization of bovine amniotic fluid derived stem cells with an underlying focus on their comparative neuronal potential at different passages. Ann. Anat. 228, 151452 https://doi: 10.1016/j.aanat.2019.151452.

Ortiz-Leal, I., Torres, M.V., Villamayor, P.R., López-Beceiro, A., Sanchez-Quinteiro, P., 2020. The vomeronasal organ of wild canids: the fox (Vulpes vulpes) as a model. J. Anat. 237, 890–906. https://doi.org/10.1111/joa.13254

Pageat, P., Gaultier, E., 2003. Current research in canine and feline pheromones. Vet. Clin. North Am. Small Anim. Pract. 33, 187–211. https://doi.org/10.1016/s0195-5616(02)00128-6

Pallé, A., Montero, M., Fernández, S., Tezanos, P., de Las Heras, J.A., Luskey, V., Birnbaumer, L., Zufall, F., Chamero, P., Trejo, J.L., 2020. Gαi2^{+} vomeronasal neurons govern the initial outcome of an acute social competition. Sci. Rep. 10, 894. https://doi.org/10.1038/s41598-020-57765-6

Papes, F., Logan, D.W., Stowers, L., 2010. The vomeronasal organ mediates interspecies defensive behaviors through detection of protein pheromone homologs. Cell 141, 692–703. https://doi.org/10.1016/j.cell.2010.03.037

Pardo-Bellver, C., Martínez-Bellver, S., Martínez-García, F., Lanuza, E., Teruel-Martí, V., 2017. Synchronized activity in the main and accessory olfactory bulbs and vomeronasal amygdala elicited by chemical signals in freely behaving mice. Sci. Rep. 7, 992424. https://doi.org/10.1038/s41598-017-10089-4

Park, C., Ahn, M., Lee, J.Y., Lee, S., Yun, Y., Lim, Y.K., Taniguchi, K., Shin, T., 2014. A morphological study of the vomeronasal organ and the accessory olfactory bulb in the Korean roe deer, Capreolus pygargus. Acta Histochem. 116, 258–264. https://doi.org/10.1016/j.acthis.2013.08.003

Perri, A., 2016. A wolf in dog's clothing: Initial dog domestication and Pleistocene wolf variation. J. Archaeol. Sci. 68, 1–4 http://dx.doi.org/10.1016/j.jas.2016.02.0030305-4403/.

Popova, N.K., 2006. From genes to aggressive behavior: the role of serotonergic system. Bioessays 28, 495–503. https://doi.org/10.1002/bies.20412

Prince, J.E., Cho, J.H., Dumontier, E., Andrews, W., Cutforth, T., Tessier-Lavigne, M., Parnavelas, J., Cloutier, J.F., 2009. Robo-2 controls the segregation of a portion of basal vomeronasal sensory neuron axons to the posterior region of the accessory olfactory bulb. J. Neurosci. 29, 14211–14222 https://doi: 10.1523/JNEUROSCI.3948-09.2009.

Ramakers, G.J., Verhaagen, J., Oestreicher, A.B., Margolis, F.L., van Bergen en Henegouwen, P.M., Gispen, W.H., 1992. Immunolocalization of B-50 (GAP-43) in the mouse olfactory bulb: predominant presence in preterminal axons. J. Neurocytol. 21, 853–869. https://doi.org/10.1007/BF01191683

Ryba, N.J., Tirindelli, R., 1997. A new multigene family of putative pheromone receptors. Neuron 19, 371–379. https://doi.org/10.1016/s0896-6273(00)80946-0

Salazar, I., Barber, P.C., Cifuentes, J.M., 1992. Anatomical and immunohistological demonstration of the primary neural connections of the vomeronasal organ in the dog. Anat. Rec. 233, 309–313. https://doi.org/10.1002/ar.1092330214

Salazar, I., Cifuentes, J.M., Sánchez-Quinteiro, P., 2013. Morphological and immunohistochemical features of the vomeronasal system in dogs. Anat. Rec. 296, 146–155. https://doi.org/10.1002/ar.22617

Salazar, I., Cifuentes, J.M., Sánchez Quinteiro, P., Garcia Caballero, T., 1994. Structural, morphometric, and immunohistological study of the accessory olfactory bulb in the dog. Anat. Rec. 240, 277–285. https://doi.org/10.1002/ar.1092400216

Salazar, I., Sánchez Quinteiro, P., 1998. Supporting tissue and vasculature of the mammalian vomeronasal organ: the rat as a model. Microsc. Res. Tech. 41, 492–505. https://doi.org/10.1002/(SICI)1097-0029(19980615)41:6<492::AID-JEMT5>3.0.CO;2-P

Salazar, I., Sánchez-Quinteiro, P., 2009. The risk of extrapolation in neuroanatomy: the case of the Mammalian vomeronasal system. Front. Neuroanat. 3, 22. https://doi.org/10.3389/neuro.05.022.2009

Salazar, I., Sánchez-Quinteiro, P., 2011. A detailed morphological study of the vomeronasal organ and the accessory olfactory bulb of cats. Microsc. Res. Tech. 74, 1109–1120. https://doi.org/10.1002/jemt.21002

Salazar, I., Sánchez-Quinteiro, P., Alemañ, N., Cifuentes, J.M., Troconiz, P.F., 2007. Diversity of the vomeronasal system in mammals: the singularities of the sheep model. Microsc. Res. Tech. 70, 752–762. https://doi.org/10.1002/jemt.20461

Salazar, I., Sanchez-Quinteiro, P., Barrios, A.W., López Amado, M., Vega, J.A., 2019. Anatomy of the olfactory mucosa. In: Handbook of Clinical Neurology. 164. Elsevier B.V., pp. 47–65. https://doi.org/10.1016/B978-0-444-63855-7.00004-6

Salazar, I., Sanchez-Quinteiro, P., Lombardero, M., Cifuentes, J.M., 2000. A descriptive and comparative lectin histochemical study of the vomeronasal system in pigs and sheep. J. Anat. 196, 15–22. https://doi.org/10.1046/j.1469-7580.2000.19610015.x

Salazar, I., Sánchez Quinteiro, P., Lombardero, M., Cifuentes, J.M., 2001. Histochemical identification of carbohydrate moieties in the accessory olfactory bulb of the mouse using a panel of lectins. Chem. Senses 26, 645–652. https://doi.org/10.1093/chemse/26.6.645

Sam, M., Vora, S., Malnic, B., Ma, W., Novotny, M.V., Buck, L.B., 2001. Neuropharmacology. Odorants may arouse instinctive behaviours. Nature 412, 142. https://doi.org/10.1038/35084137

Shapiro, L.S., EE, P.L., Halpern, M., 1995. Lectin histochemical identification of carbohydrate moieties in opossum chemosensory systems during development, with special emphasis on VVA-identified subdivisions in the accessory olfactory bulb. J. Morphol. 224, 331–349. https://doi.org/10.1002/jmor.1052240307

Shibata, S., Cho, K.H., Kim, J.H., Abe, H., Murakami, G., Cho, B.H., 2013. Expression of hyaluronan (hyaluronic acid) in the developing laminar architecture of the human fetal brain. Ann. Anat. 19, 424–430. https://doi.org/10.1016/j.aanat.2013.07.002

Skoglund, P., Ersmark, E., Palkopoulou, E., Dalén, L., 2015. Ancient wolf genome reveals an early divergence of domestic dog ancestors and admixture into high-latitude breeds. Curr. Biol. 25, 1515–1519. https://doi.org/10.1016/j.cub.2015.04.019

Sundman, A.S., Pértille, F., Lehmann Coutinho, L., Jazin, E., Guerrero-Bosagna, C., Jensen, P., 2020. DNA methylation in canine brains is related to domestication and dog-breed formation. PloS One 15, e0240787. https://doi.org/10.1371/journal.pone.0240787

Switzer 3rd, R.C., Johnson, J.I., Kirsch, J.A., 1980. Phylogeny through brain traits. Relation of lateral olfactory tract fibers to the accessory olfactory formation as a palimpsest of mammalian descent. Brain Behav. Evol. 17, 339–363. https://doi.org/10.1159/000121808

Takigami, S., Mori, Y., Ichikawa, M., 2000. Projection pattern of vomeronasal neurons to the accessory olfactory bulb in goats. Chem. Senses 25, 387–393. https://doi.org/10.1093/chemse/25.4.387

Tolivia, J., Tolivia, D., Navarro, A., 1988. New technique for differential staining of myelinated fibers and nerve cells on paraffin sections. Anat. Rec. 222, 437–440. https://doi.org/10.1002/ar.1092220416

Torres, M.V., Ortiz-Leal, I., Villamayor, P.R., Ferreiro, A., Rois, J.L., Sanchez-Quinteiro, P., 2020. The vomeronasal system of the newborn capybara: a morphological and immunohistochemical study. Sci. Rep. 10, 13304. https://doi.org/10.1038/s41598-020-69994-w

Torres, M.V., Ortiz-Leal, I., Villamayor, P.R., Ferreiro, A., Rois, J.L., Sanchez-Quinteiro, P., 2021. Does a third intermediate model for the vomeronasal processing of information exist? Insights from the macropodid neuroanatomy. Brain Struct. Funct. 2. https://doi.org/10.1007/s00429-021-02425-

Trinh, K., Storm, D.R., 2003. Vomeronasal organ detects odorants in absence of signaling through main olfactory epithelium. Nat. Neurosci. 6, 519–525. https://doi.org/10.1038/nn1039

Trut, L., Oskina, I., Kharlamova, A., 2009. Animal evolution during domestication: the domesticated fox as a model. Bioessays 31, 349–360. https://doi.org/10.1002/bies.200800070

Vigne, J.D., Guilaine, J., Debue, K., Haye, L., Gérard, P., 2004. Early taming of the cat in Cyprus. Science 304, 259. https://doi.org/10.1126/science.1095335

Villamayor, P.R., Cifuentes, J.M., Quintela, L., Barcia, R., Sanchez-Quinteiro, P., 2020. Structural, morphometric and immunohistochemical study of the rabbit accessory olfactory bulb. Brain Struct. Funct. 225, 203–222. https://doi.org/10.1007/s00429-019-01997-4

Wang, G., Shi, P., Zhu, Z., Zhang, Y.P., 2010. More functional V1R genes occur in nest-living and nocturnal terricolous mammals. Genome Biol. Evol. 2, 277–283. https://doi.org/10.1093/gbe/evq020

Wang, X., Pipes, L., Trut, L.N., Herbeck, Y., Vladimirova, A.V., Gulevich, R.G., Kharlamova, A.V., Johnson, J.L., Acland, G.M., Kukekova, A.V., Clark, A.G., 2018. Genomic responses to selection for tame/aggressive behaviors in the silver fox (Vulpes vulpes). Proc. Natl. Acad. Sci. USA 115, 10398–10403. https://doi.org/10.1073/pnas.1800889115

Wekesa, K.S., Anholt, R.R., 1999. Differential expression of G proteins in the mouse olfactory system. Brain Res. 837, 117–126. https://doi.org/10.1016/s0006-8993(99)01630-3

Wyatt, T.D., 2003. Pheromones and Animal Behaviour: Communication by Smell and Taste. Cambridge University Press, Cambridge.

Wysocki, C.J., 1979. Neurobehavioral evidence for the involvement of the vomeronasal system in mammalian reproduction. Neurosci. Biobehav. Rev. 3, 301–341. https://doi.org/10.1016/0149-7634(79)90015-0

Young, J.M., Trask, B.J., 2007. V2R gene families degenerated in primates, dog and cow, but expanded in opossum. Trends Genet. 23, 212–215. https://doi.org/10.1016/j.tig.2007.03.004

Zeder, M.A., 2012. Pathways to animal domestication. In: Gepts, P. (Ed.), Biodiversity in Agriculture: Domestication, Evolution and Sustainability. Cambridge Univ. Press, Cambridge, UK, pp. 227–259.

Zimmerman, A.D., Munger, S.D., 2021. Olfactory subsystems associated with the necklace glomeruli in rodents. Cell Tissue Res. 383, 549–557. https://doi.org/10.1007/s00441-020-03388-2